Nanostructured lipid carriers loaded into in situ gels for breast cancer local treatment

Julia S. Passos , Alexsandra C. Apolinario , Kelly Ishida , Tereza S. Martins , Luciana B. Lopes

PII: S0928-0987(23)00268-3
DOI: https://doi.org/10.1016/j.ejps.2023.106638
Reference: PHASCI 106638

To appear in: *European Journal of Pharmaceutical Sciences*

Received date: 4 July 2023
Revised date: 18 October 2023
Accepted date: 11 November 2023

Please cite this article as: Julia S. Passos , Alexsandra C. Apolinario , Kelly Ishida , Tereza S. Martins , Luciana B. Lopes , Nanostructured lipid carriers loaded into in situ gels for breast cancer local treatment, *European Journal of Pharmaceutical Sciences* (2023), doi: https://doi.org/10.1016/j.ejps.2023.106638

Nanostructured lipid carriers loaded into *in situ* gels for breast cancer local treatment

Julia S. Passos[1], Alexsandra C. Apolinario[1], Kelly Ishida[2], Tereza S. Martins[3], Luciana B. Lopes[1]*

[1] Department of Pharmacology, Institute of Biomedical Sciences, University of Sao Paulo, Brazil

[2] Department of Microbiology, Institute of Biomedical Sciences, University of Sao Paulo, São Paulo, Brazil

[3] Department of Chemistry, Federal University of Sao Paulo (UNIFESP), Diadema, São Paulo, Brazil

***Corresponding author:** *Luciana B. Lopes*, Pharmacology Department, Institute of Biomedical Sciences, University of Sao Paulo, 1524 Av. Prof. Lineu Prestes, Sao Paulo-SP 05508-000, Brazil. E-*mail address*: lublopes@usp.br

Abstract

In this study, nanostructured lipid carriers (NLC) were developed and employed to obtain *in situ* thermosensitive formulations for the ductal administration and prolonged retention of drugs as a new strategy for breast cancer local treatment. NLC size was influenced by the type and concentration of the oil phase, surfactants, and drug incorporation, ranging from 221.6 to 467.5 nm. The type of liquid lipid influenced paclitaxel and 5-fluorouracil cytotoxicity, with tributyrin-containing NLC reducing IC_{50} values by 2.0-7.0-fold compared to tricaprylin NLC in MCF-7, T-47D and MDA-MB-231 cells. In spheroids, the NLCs reduced IC_{50} compared to either drug solution (3.2–6.2-fold). Although a significant reduction (1.26 points, $p<0.001$) on the health index of *Galleria mellonella* larvae was observed 5 days after NLC administration, survival was not significantly reduced. To produce thermosensitive gels, the NLCs were incorporated in a poloxamer (11%, w/w) dispersion, which gained viscosity (2-fold) at 37°C. After 24 h, ~53% of paclitaxel and 83% of 5-fluorouracil were released from the NLC; incorporation in the poloxamer gel further prolonged release. Intraductal administration of NLC-loaded gel increased the permanence of hydrophilic (2.2-3.0-fold) and lipophilic (2.1-2.3-fold) fluorescent markers in the mammary tissue compared to the NLC (as dispersion) and the markers solutions. In conclusion, these results contribute to improving our understanding of nanocarrier design with increased cytotoxicity and prolonged retention for the intraductal route. Tributyrin incorporation increased the cytotoxicity of paclitaxel and 5-fluorouracil in monolayer and spheroids, while NLC incorporation in thermosensitive gels prolonged tissue retention of both hydrophilic and hydrophobic compounds.

Keywords: lipid nanoparticles; intraductal; breast cancer; thermosensitive gel; paclitaxel; 5-fluorouracil

1. Introduction

Ductal carcinoma *in situ* (DCIS) is a heterogeneous breast cancer phenotype that arises in the epithelium of ducts and represents 20-25% of breast tumors (Badve and Gökmen-Polar 2019). Despite being considered a local form of breast cancer by several authors, its treatment is aggressive and involves surgery, radiotherapy and long-term endocrinotherapy due to the risk of progression to invasive forms (Badve and Gökmen-Polar 2019, van Seijen, Lips et al. 2019). However, this standard of care has been criticized for low-grade DCIS and stimulated the scientific community to explore less invasive management strategies (Narod, Iqbal et al. 2015, Groen, Elshof et al. 2017, Sagara, Julia et al. 2017). Among them, the intraductal administration of cytotoxic drugs has attracted attention (Sapienza Passos, Dartora et al. 2023).

Intraductal therapy can be defined as drug delivery directly into the mammary ducts through the nipples (Murata, Kominsky et al. 2006, Stearns, Mori et al. 2011, Kuang, Liu et al. 2020). Since DCIS originates in the ductal epithelium, the intraductal route allows increased local exposure to the drug (Mahoney, Gordon et al. 2013, Sapienza Passos, Dartora et al. 2023). It has been pre-clinically and/or clinically employed for administration of paclitaxel, curcumin, methotrexate, piplartine and doxorubicin, among other compounds (Okugawa, Yamamoto et al. 2005, Chun, Bisht et al. 2012, Kuang, Liu et al. 2020, Gao, Liu et al. 2021, Dartora, Salata et al. 2022, Salata and Lopes 2022). These studies demonstrated the possibility of cannulating the affected mammary ducts of patients with DCIS in a well-tolerated and safe manner and provided strong evidence that intraductal drug administration results in therapeutic responses with reduced systemic adverse effects. Despite its promises, several challenges related to duct cannulation, perforation and personnel training have been reported (Singh, Gao et al. 2012, Gu, Gao et al. 2018, Kuang, Liu et al. 2020), highlighting the need to develop local formulations that prolong drug retention in the mammary tissue and enable reduction of the administration frequency to improve the acceptance and widen the

application of this promising route (Joseph, Islam et al. 2020, Patil, Narvenker et al. 2020). Nanocarriers (like polymeric nanoparticles and nanoemulsions) and other delivery systems were proposed to fulfill this need (Carvalho, Salata et al. 2019, Joseph, Islam et al. 2020, Salata and Lopes 2022, Sapienza Passos, Dartora et al. 2023). Recently, it has been demonstrated that fluorescence of hydrophilic markers in the breast declined more slowly after administration of a PLGA (poly(lactic-co-glycolic acid) gel compared to nanoparticles (Joseph, Islam et al. 2020), which led us to hypothesize that incorporation of nanocarriers in *in situ* gels could further prolong tissue retention of drugs while aiding cytotoxicity. Thus, the main goal of the present study was to combine the advantages of nanostructured lipid carriers (NLC) and thermosensitive gels and develop a new nanotechnology-based system for the intraductal delivery of hydrophilic and hydrophobic cytotoxic drugs and local treatment of breast cancer. The NLC was selected based on previous studies demonstrating (i) its ability to prolong drug release, which is interesting for a local delivery approach, (ii) its incorporation into pharmaceutical dosage forms (including gels) without losing integrity and (iii) the possibility to include other lipids in the matrix that might aid cytotoxicity (Shamma and Aburahma 2014, Migotto, Carvalho et al. 2018, Garg, Tandel et al. 2021, Lanna, Siqueira et al. 2021).

In the first part of the study, the impact of surfactants, liquid lipid and drug properties on NLC characteristics and cytotoxic properties was assessed. Although the optimization of NLC properties has been examined for systemic therapy (Pedro, Almeida et al. 2019, Poonia, Kaur Narang et al. 2019, Chand, Kumar et al. 2021, Gadag, Narayan et al. 2021), NLC development taking into consideration the characteristics and aims of intraductal administration is missing. Paclitaxel and 5-fluorouracil were selected as model cytotoxic compounds with varying physicochemical characteristics. Their incorporation separately in the NLC enabled us to assess the effects of NLC on the cytotoxicity and mammary retention

of compounds with varying lipophilicity but still potentially employed for breast cancer treatment. Although treatment of breast cancer varies with the type, stage and histopathological characteristics, most guidelines include 5-fluorouracil and paclitaxel in chemotherapy regimens (Fujii, Le Du et al. 2015, Korde, Somerfield et al. 2021). For example, doxorubicin and cyclophosphamide for 4 cycles followed by paclitaxel for 4 cycles is frequently employed in the United States (Moo, Sanford et al. 2018), while fluorouracil-containing regimens have been accepted in sequential combination with taxanes (Fujii, Le Du et al. 2015, Del Mastro, Poggio et al. 2022). Paclitaxel stops cell division by β-tubulin binding and stabilization of microtubules. Despite the broad spectrum of efficacy, its use is limited by its toxicity and high lipophilicity (log P = 3.2 and MW = 853.9 g/mol), which represents a challenge for formulation development and bioavailability (Gradishar 2006, Marupudi, Han et al. 2007, Jain, Kumar et al. 2012, Weaver 2014, Bernabeu, Cagel et al. 2017, NCBI 2022). 5-Fluorouracil (5-FU), in turn, is a hydrophilic (log P = -0.89 and MW = 130.1 g/mol) antimetabolite analogue of uracil, which acts by erroneous incorporation into RNA and interruption of its processing and assembly (Longley, Harkin et al. 2003, NCBI 2021), and inhibition of thymidylate synthase, the only source of thymidylate for DNA replication and repair (Longley, Harkin et al. 2003).

In the second part of the study, we investigated the NLC incorporation into poloxamer 407 thermosensitive dispersions. This polymer undergoes a sol-gel transition at ~34°C by desolvation and aggregation of its hydrophobic chains (Dewan, Bhowmick et al. 2015, Soliman, Ullah et al. 2019), and has been demonstrated to increase the local retention of drugs after their intravaginal, ocular and intravesical administration (Ci, Huang et al. 2017, Yoon, Chang et al. 2019). Because it is fluid at room temperature, we hypothesized that the NLC-loaded poloxamer dispersion would be easily administered through the ducts, but its gelation at body temperature could prolong mammary tissue retention. After formulation

optimization, assessment of *in vivo* mammary tissue retention and local irritation, formulation safety and stability were investigated.

2. Materials and Methods

2.1 Materials

Polysorbate 80 (Tween 80), sorbitan oleate (Span 80), tributyrin, decyl glucoside and poloxamer 407 (Pluronic 127) were obtained from Sigma (St. Louis, MO, USA). Paclitaxel was purchased from Cayman Chemical (Ann Arbor, MI, USA) and soy phosphatidylcholine (PC) and 1-palmitoyl-2-(6-((7-nitro-2-1,3-benzoxadiazol-4-yl)amino)hexanoyl)-sn-glycero-3-phosphocholine (NBD-PC) were purchased from Avanti Polar Lipids (Alabaster, AL, USA). 5-Fluorouracil were obtained from Oakwood Chemical (Estill, SC, USA). Rhodamine B and propylene glycol were acquired from Synth (São Paulo, SP, Brazil) and Alexa Fluor 647 was obtained from ThermoFisher Scientific (Waltham, MA, USA). Tricaprylin was kindly supplied by Croda Health Care (Edison, NJ, USA), and glyceryl behenate (Compritol® 888 ATO) by Gattefosse (Saint-Priest, France). Ultrapure water was used unless stated in the individual methods.

2.2 Formulation design and development

As the general procedure to obtain NLC, the fusion emulsification technique was employed (Passos, Martino et al. 2020). The solid lipid (glyceryl behenate), liquid lipid and oil phase surfactant were mixed, and melted at 80 °C. Once the solid lipid was completely melted, the heated aqueous phase containing the hydrophilic surfactant was added into the oil phase under vortex stirring. The resulting system was sonicated in a water bath at room temperature in pulses (50 s on and 30 s off) and 40% amplitude (VCX500, Sonics, Newtown, CT). To this general procedure, several modifications were included to investigate the

influence of the NLC components on the nanocarrier characteristics as described in the subsequent subsections and summarized in the **Supplementary Table S1**.

2.2.1. Influence of the liquid oil and oil phase surfactant types: the starting point was the NLC previously characterized by our group (Passos, Martino et al. 2020), in which Span 80 and tricaprylin were employed as hydrophobic surfactant and liquid lipid, respectively. Our first goal was to understand the effects of replacing Span 80 with phosphatidylcholine as surfactant, which has been previously associated with low local irritation, increased tumor cell uptake, and easier surface functionalization (Vater, Apanovic et al. 2021, Wünsch, Mulac et al. 2021, Zhan, Yi et al. 2021). A second goal was to assess whether tricaprylin could be replaced by tributyrin as liquid lipid, since this triglyceride has been demonstrated to potentiate the cytotoxicity of drugs against cancer cells (Carvalho, Migotto et al. 2017, Salata and Lopes 2022, Fukumori, Branco et al. 2023). To the mixture of glyceryl behenate with tricaprylin or tributyrin (comprising 10% w/w of the total formulation), we added the oil phase surfactant (either Span 80 or phosphatidylcholine at 3%, w/w), and the system was melted at 80 °C. The heated aqueous phase containing polysorbate 80 (3% w/w, comprising 90% of the total amount of formulation) was subsequently added under vortex stirring. The resulting system was sonicated in pulses (50 s on and 30 s off) and 40% amplitude for 10 or 20 min to assess the influence of sonication time on particle diameter.

2.2.2. Influence of the aqueous phase surfactant concentration and type: to try to reduce surfactant content, NLC production was investigated using the aqueous phase containing 1% (w/w) of either polysorbate 80 or decyl glucoside as surfactant, which was added to the mixture of glyceryl behenate and tributyrin. The system was sonicated for 20 min in pulses (50 s on and 30 s off) and 40% amplitude.

2.2.3. Influence of drug type and content: since one of our aims was to compare the NLC ability to incorporate, prolong mammary retention and increase the cytotoxicity of drugs with varying physicochemical characteristics, the influence of paclitaxel and 5-FU concentration on NLC characteristics was assessed. For drug-loaded nanocarriers, paclitaxel was dissolved in the oil phase, while 5-FU was dispersed in the oil phase surfactant (prior to addition into the oil phase). The drugs were incorporated separately in the NLCs. The aqueous phase was subsequently added, and the mixture was probe sonicated; two drug concentrations (0.5 and 1.0%, w/w) were evaluated.

After each of these methodological variations, a formulation was selected according to a desired size rage and PDI. Although previous studies suggest that smaller nanoparticles result in lower retention (Singh, Gao et al. 2012, Gu, Gao et al. 2018, Joseph, Islam et al. 2020), the upper diameter limit that can maximize retention without causing duct obstruction has not been defined. Because ductal diameter changes with location, we set the desired diameter at 200-500 nm to prolong retention without compromising safety. The second desired characteristic was PDI below 0.30 for low polydispersity (Danaei, Dehghankhold et al. 2018).

2.3. Nanocarrier characterization

2.3.1. Size distribution, zeta potential and morphology

For nanocarrier characterization, particle size, polydispersity index (PDI) and zeta potential were measured at 25°C using a Malvern Zetasizer NanoZS90 equipment (Malvern Instruments Ltd., UK). The NLC were diluted with ultrapure water at 1:100 (v/v), and 3

individual measurements of each formulation batch were obtained. Results were expressed as average ± standard deviation.

To confirm the results from dynamic light scattering (DLS) and evaluate the morphological aspects of the nanocarriers, the formulations were analyzed by scanning electron microscopy (SEM). The samples were diluted with distilled water (1:500, v/v) and placed in a glass coverslip to dry overnight at room temperature (Passos, Martino et al. 2020). All samples were placed on stubs of aluminum and metalized with platinum before visualization under a Quanta FEG 650 scanning electron microscope (FEI Company, Hillsborough, OR, USA, located at the Polytechnic School, University of São Paulo).

2.3.2. Thermal analysis

Thermal analysis was performed to characterize the liquid lipid influence on the solid lipid crystallinity and melting point, as well as drug solubilization in the nanocarrier matrix. To conduct differential scanning calorimetry (DSC) and thermogravimetric analysis (TGA), the simultaneous thermal analyzer Discovery SDT 650 (TA Instruments, Delaware, USA) was employed. Samples of 7 - 10 mg were subjected to a heating rate from room temperature (25 °C) to 500 °C at 10 °C/min, under nitrogen atmosphere (100 mL/min), using an alumina crucible (90 µL) (Passos, Martino et al. 2020, Losito, Lopes et al. 2021). Analyzes were performed for the following samples: liquid lipid, solid lipid, a physical mixture of liquid and solid lipids (with and without drugs) in the ratios used in the optimized formulation and lyophilized drug-loaded or unloaded nanocarriers.

2.4 Effects of the formulation on cell viability

2.4.1 Cell culture

Breast cancer cells (MCF-7, T-47D and MDA-MB-231) and non-tumoral mammary cells (MCF-10A) were obtained from ATCC (Manassas, VA, USA). Breast cancer cells were cultured in Dulbecco's Modified Eagle Medium:Nutrient Mixture F-12 (DMEM-F12) culture medium supplemented with 10% fetal bovine serum (FBS, Gibco/Invitrogen, USA), 50 μg/mL penicillin, 50 μg/mL streptomycin, and 0.5 μg/mL amphotericin. MCF-10A cells were cultured in DMEM - GlutaMAX™ (Gibco, Carlsbad, CA) medium supplemented with 5% horse serum (Gibco, Carlsbad, CA), 0.1 μg/mL cholera toxin, 10 μg/mL insulin, 0.5 μg/mL g/mL hydrocortisone, 0.02 μg/mL Epidermal Growth Factor, and 1% penicillin and streptomycin (100 U/mL and 100 μg/mL Gibco, Carlsbad, CA). Cells were maintained at 37 °C and 5% CO_2 atmosphere.

2.4.2 Cytotoxic effects of the nanocarrier in cell monolayers (2D model)

To assess the cytotoxic effects of the nanocarriers, the MTT (3-[4,5-dimethylthiazol-2-yl]-2,5 diphenyl tetrazolium bromide) assay was used (Apolinário, Salata et al. 2022, Salata and Lopes 2022). Cells (T-47D, MCF-7, MDA-MB-231 and MCF-10A) were seeded (5×10^4 cells per well) in 96-well micro-plates containing 200 μL of DMEM-F12 medium and allowed to attach for 24 h. After overnight incubation, cells were treated with formulations at concentrations in the range of 0.003 – 50 mg/mL. After 72 h of treatment, the culture medium was removed and replaced by 150 μL of the MTT dye solution (0.5 mg/mL) for 3 h. Next, the medium was removed from each well, and an equal amount of dimethyl sulfoxide (DMSO) was added. Absorbance was measured in a plate reader at 595 nm and drug effect was calculated in relation to a negative control (untreated cells).

2.4.3 Cytotoxic effects of the nanocarrier in spheroids (3D model)

Spheroids of MCF-7 and T-47D were obtained using the liquid overlay technique (Salata, Malagó et al. 2021, Salata and Lopes 2022). Round bottom 96-well microplates were coated with an agarose gel at 1% (50 µL/well) before seeding the cells at 5×10^3 cells/well. Next, the plates were centrifuged at 1000 rpm for 7 min and incubated at 37°C in a 5% CO_2 atmosphere. After 5 days of incubation, the spheroids were treated with serial dilutions of drug solutions, unloaded nanocarriers (NLC without paclitaxel or 5-FU) and drug-loaded nanocarriers for 72 h. After treatment, spheroid viability was assessed using the CellTiterGlo® 3D kit (Promega, Madison, WI, USA) and luminescence (recording at 560 nm) as previously described (Salata, Malagó et al. 2021). The morphology of MCF-7 and T-47D spheroids was evaluated using a Nikon Eclipse TE300 microscope (Melville, NY, USA) on days 1 and 5 after incubation (before treatment), as well as after treatment for 72 h with NLC-TB-P and NLC-TB-5FU at their respective IC_{50} values.

2.5 Evaluation of biosafety in Galleria mellonella model

To estimate safety of unloaded nanocarriers (without paclitaxel or 5-FU) prior to administration in rats, the *Galleria mellonella* model was employed (Migotto, Carvalho et al. 2018, Passos, Martino et al. 2020). Healthy larvae (2.0 – 2.5 cm in length and 150 – 200 mg of body weight) were selected and separated into experimental groups of 16 larvae. An aliquot of 10 µL of unloaded NLC or PBS (negative control) was administered at the last left pro-leg of the larvae, which were incubated in Petri dishes containing beeswax and pollen at 37 °C. Survival and health status were assessed daily for up to 5 days; high health indexes and survival rates indicated low toxicity and safety of the formulation.

2.6 Nanocarrier incorporation into a thermosensitive gelling system

The first step was to select the concentration of Poloxamer 407 to obtain a fluid gel at biologically relevant temperatures while remaining liquid at room temperature (to facilitate intraductal administration). Poloxamer 407 dispersions were obtained by adding an appropriate amount of poloxamer (1 – 20%, w/w) in distilled water while stirring, and allowing the samples to rest overnight in the refrigerator (4 °C) for poloxamer dissolution. To obtain a formulation with appropriate viscosity for intraductal administration that gained viscosity in vivo to improve retention time in the breast, the sol-gel transition temperature was studied using the test-tube inversion method (Yoon, Chang et al. 2019). Briefly, glass vials containing 2 mL of each formulation were placed in a water bath and heated at a rate of 3 °C every 5 minutes from 4 °C to 40 °C. The gelation temperature was set as the temperature at which the solution lost fluidity.

Selected poloxamer solutions (11 – 15%, w/w) were evaluated for their rheological behavior and viscosity using a cone-plate rheometer (RST-CPS Cone/Plate equipped with Rheo3000 software, Brookfield, Massachusetts, USA) and a bath circulator (TC-650, Brookfield Engineering Laboratories, Massachusetts, USA) (Apolinário, Salata et al. 2022). Samples were maintained at 25 or 37 °C and the shear rate was varied in the range of 0 - 2000 1/s. To classify the fluid behavior, the Power law equation was used ($\tau=K\gamma n$), in which τ = shear stress, K = consistency index, γ = shear rate and n = flow index (Barnes 1989, Sinko 2011, Hosmer, Steiner et al. 2013). In this model, the value of n indicates the type of behavior, and when n=1 it is a Newtonian fluid, n>1 it is a dilatant fluid, and n<1 it is a pseudoplastic fluid. The analysis was performed using the Origin 2018 software. Poloxamer at 11% (w/w) was selected as the optimal polymer concentration.

For NLC incorporation in the selected poloxamer dispersion, optimized nanocarrier formulations were freeze-dried using trehalose as cryoprotectant (Khan, Mudassir et al. 2019, Karakash, Vasileska et al. 2020). A trehalose solution at 10% was added to the NLC

formulation (1:1, v/v) and the mixture was frozen at -20°C for 12 hours, followed by 24 hours of drying (vacuum and temperature of -50°C, FreeZone 2.5, Labconco). Freeze-dried nanocarriers were resuspended to the initial volume of the formulation (0.5 mL) in poloxamer solutions and vortexed until a homogeneous dispersion was obtained. The NLC dispersion as obtained will be referred to as "NLC aqueous dispersion", while the NLC incorporated in poloxamer will be referred to as "NLC poloxamer dispersion".

2.7 Changes on NLC characteristics and drug encapsulation upon short-term storage

To estimate stability, a preliminary study was performed to assess changes as a function of time on the characteristics of the optimized nanocarriers as obtained (NLC aqueous dispersion), after freeze-drying and as poloxamer dispersion. The samples were stored at room temperature (25 °C) in conical vials. At days 0 (immediately after production), 7, 15, 30, 45 and 60, formulation evaluation was performed, both macroscopically (coalescence and/or gravitational separation) and microscopically (analysis of size distribution and zeta potential) (Passos, Martino et al. 2020). Particle size, polydispersity index (PDI) and zeta potential were assessed using a Malvern Zetasizer NanoZS90 equipment (Malvern Instruments Ltd., UK). The NLC dispersion was diluted with ultrapure water at 1:100 and 1:1000 (v/v, with no significant difference in the values of diameter obtained), while the poloxamer dispersion containing NLC was diluted at 1:1000 (v/v). The unloaded poloxamer dispersion (no NLC) was diluted at the same ratio and employed as a control for interference, i.e., to ensure that there were no particles with the same size distribution as the NLC. Three individual measurements of each formulation batch were obtained, and results were expressed as the average ± standard deviation.

We also assessed changes in the encapsulation efficiency of paclitaxel and 5-fluorouracil at days 30 and 60. For freeze-dried nanoparticles, redispersion in water (to obtain

the same volume as before freeze-drying) was performed before evaluation. Drug encapsulation was evaluated indirectly by the ultrafiltration method as previously described (Passos, Martino et al. 2020). Samples were diluted in MilliQ water (1:2, v/v) and placed in the upper chamber of an Amicon Ultra 4 centrifugal filter (Millipore Corporation, USA). The diluted formulations were centrifuged for 1h at 4000 rpm (Eppendorf, mod. 5430R, Hamburg, Germany) and the filtrate was collected for drug quantification by HPLC. The encapsulation efficiency (EE%) was calculated using the equation $EE\% = (W_{initial\ drug} - W_{free\ drug})/ W_{initial\ drug} \times 100$, where $W_{initial\ drug}$ is the drug amount used for NLC obtainment and $W_{free\ drug}$ is the amount of free drug quantified in the filtrate.

2.8 Evaluation of in vitro drug release

Paclitaxel and 5-fluorouracil release from the NLC–loaded poloxamer dispersion was compared to the NLC aqueous dispersions using Franz diffusion cells for 24 h. Because the poloxamer dispersion gains viscosity at 37°C (see results), and the assay was conducted at this temperature, the gel was formed *in situ* at the beginning of the experiment. One hundred and fifty microliters of each formulation were placed in the donor compartment and separated from the receptor phase (phosphate buffer, pH 7.4, with or without 20% ethanol, for paclitaxel and 5-FU, respectively) using a cellulose dialysis membrane (MWCO 14,000 Da, Sigma-Aldrich, St. Louis, MO, USA). The drug solutions were employed as controls to ensure that they could diffuse through the membrane and dissolve in the receptor phase (Mekjaruskul, Beringhs et al. 2021, Salata and Lopes 2022). The system was maintained at 37°C under stirring (350 rpm) and, at specific intervals, 300 µL of the receptor phase was withdrawn and replaced with 300 µL of fresh receptor phase.

Drug quantification was performed using High-Performance Liquid Chromatography (HPLC) (Carvalho, Migotto et al. 2017, Hanif, Akhtar et al. 2018, Fukumori, Branco et al.

2023). Briefly, separation of paclitaxel was performed on a Shimadzu HPLC system (SCL-10A VP) equipped with a Phenomenex C18 column (150 x 4.6 mm) and a mobile phase composed of acetonitrile:water (6:4, v/v) at a flow rate of 1.0 mL/min and detection at 228 nm at room temperature (25°C) (Carvalho, Migotto et al. 2017). Linearity was observed within the range of 0.05 to 50 µg/mL, with a limit of quantification of 0.2 µg/mL (Hosmer, Shin et al. 2011, Carvalho, Migotto et al. 2017). 5-Fluorouracil was quantified on a Shimadzu LC2030C 3D system with a Phenomenex C18 column (150 x 4.6 mm) and mobile phase composed of a 10mM acetic acid solution and acetonitrile at 98:2 (v/v), at a flow rate of 1.0 mL/min and detection at 265 nm (Hanif, Akhtar et al. 2018, Fukumori, Branco et al. 2023). Linearity was observed at 0.1 - 20 µg/mL, with a quantification limit of 0.3 µg/mL.

For evaluation of release kinetics, the amount of drug released was fitted to different models: zero-order kinetics ($Q_t = Q_0 + K_0 t$), Higuchi kinetics ($Q = K_h t^{1/2}$) and first-order kinetics ($\log Q_t = -K_t/2303 + \log Q_0$). On those models, Q_t represents the amount of drug released in t (time in hours), Q_0 is the initial amount of drug, K_0 is a zero-order kinetic constant and K_h, the Higuchi dissolution constant (Costa and Lobo 2001, Jain and Jain 2016).

2.9 Evaluation of in vivo mammary tissue retention

2.9.1 Animals

Female Wistar rats (6 weeks) were obtained from the Animal Facility for the Production of Rats of the Institute of Biomedical Sciences of the University of São Paulo (ICB-USP) and housed in the Animal Facility of the Department of Pharmacology with free access to food and water. The room was kept at a temperature range of 22 - 23 °C under a 12-hour light-dark cycle. All experiments were conducted according to the guidelines of the National Council for Animal Experimentation (CONCEA) and approved by the Animal Care and Use Committee of the ICB-USP.

2.9.2 Intraductal administration and local retention of a fluorescent marker

The aims of this experiment were (i) to compare the mammary tissue retention of lipo- and hydrophilic fluorescent markers (rhodamine B and Alexa Fluor 647, respectively) incorporated into NLCs and administered via intraductal or systemic routes (i.p), and (ii) to assess whether nanocarrier incorporation in the poloxamer dispersion increased the residence time of the markers compared to simple solutions (in propylene glycol and water, for rhodamine and Alexa Fluor, respectively) and the NLC aqueous dispersion. Nanocarriers containing rhodamine (0.05%, w/w) or Alexa Fluor (0.01%, w/w) were prepared by replacing the drugs in the optimized formulation with the markers: rhodamine was dissolved in the oil phase while Alexa Fluor was dispersed in the oil phase surfactant prior to addition into the oil phase. Both fluorescent markers-loaded NLCs were obtained with 10% of oil phase (glyceryl behenate and tributyrin, 1:1), 6% of surfactants (Span 80 and polysorbate 80, 1:1), and 84% of PBS, and were probe sonicated for 20 minutes protected from light.

For intraductal administration, rats were anesthetized with isoflurane (2 – 2.5%, by inhalation) and abdominal hair was removed using a depilatory cream (Migotto, Carvalho et al. 2018, Carvalho, Salata et al. 2019, Salata and Lopes 2022). After 24 h, the nipples were gently rubbed with gauze soaked in 70% alcohol to reveal the duct orifices, and the treatments were intraductally administered (20 µL, 33G needle, Hamilton, Bonaduz, Switzerland) to three pairs of nipples; intraperitoneal (i.p) injection was used as a control of systemic administration. The *in vivo* fluorescence intensity was assessed using the IVIS Spectrum system (Perkin-Elmer Life Sciences, Waltham, MA, USA, CEFAP-ICB-USP) for up to 120 h. The following instrument settings were fixed for comparison among groups: exposure time = 0.5 s, binning factor = 8 – 2 and excitation/emission = 465/540 nm

(rhodamine B) or 640/780 nm (Alexa Fluor 647). To ensure that fluorescence was related to the markers, unloaded nanocarriers were administered as controls.

To assess formulation-mediated histological changes, the mammary tissue was excised, fixed in 10% formaldehyde and embedded in paraffin for sectioning (5 µm) and staining (with hematoxylin/eosin) prior to microscopic analysis. In each section, the infiltration of inflammatory cells and changes in the morphology of the ductal and lobular units were studied (Carvalho, Salata et al. 2019, Salata and Lopes 2022). In addition to local irritation evaluation, blood samples were collected from the left ventricle of the rats, at the time of euthanasia, in tubes containing EDTA, to perform blood smears and differential leukocyte counts.

2.10 Statistical analysis

The results are reported as means ± standard deviation or means ± standard error. Data were statistically analyzed using t test or ANOVA followed by Tukey post hoc test (GraphPad Prism Software, California, USA). Values were considered significantly different when $p<0.05$.

3. Results

3.1 Nanostructured lipid carrier development and optimization

Particles obtained with Span 80 as surfactant and sonicated by 10 min displayed a similar size whether tricaprylin or tributyrin were employed as liquid lipid (**Figure 1 A**). Increasing the sonication time to 20 min reduced particle diameter only by 1.1 and 1.2-fold for tributyrin and tricaprylin, respectively. When Span was replaced by PC and sonication time was maintained at 10 min, a significant ($p < 0.0001$) increase in the diameter of tributyrin-containing NLC (388.8 nm) compared to tricaprylin-containing NLC (221.6 nm)

was observed. Increasing sonication time to 20 min reduced (by 1.3-fold) the diameter of tributyrin-containing NLC, and it became similar to that containing tricaprylin.

All nanoparticles showed homogeneous size distribution, regardless of the choice of formulation components and sonication time (denoted by a PDI < 0.25). Additionally, all NLCs were negatively charged (-9.3 to – 25.5 mV). NLC obtained with tricaprylin showed significantly lower Zeta potential values ($p < 0.0019$ and 0.0001) compared to NLC obtained with tributyrin. For particles obtained with tricaprylin as liquid lipid, using Span 80 as surfactant further reduced the Zeta potential of the formulation. Therefore, based on the results, to use phosphatidylcholine as a surfactant and tributyrin as the liquid lipid (aiming at enhancing the cytotoxic effect), longer sonication times were required to achieve the desired size.

In the second round of formulation modifications, we assessed the effect of type and concentration of the aqueous phase surfactant (**Figure 1 B**) when NLCs were produced using PC at 3% as oil phase surfactant, tributyrin as liquid lipid and sonication for 20 min. Nanoparticles obtained with 3% of surfactants in the aqueous phase showed reduced size, regardless of whether Tween 80 or decyl glycoside was used. Reducing the surfactant concentration to 1% increased the particle size significantly (1.6- and 2.6-fold for NLC obtained with Tween 80 and decyl glucoside, respectively, $p < 0.01$ or 0.0001) and increased the PDI in samples obtained with decyl glucoside (from 0.22 to 0.35, $p < 0.0001$). At 3%, the aqueous phase surfactants reduced the Zeta potential, an effect that was more pronounced with decyl glucoside (2.2-fold, $p < 0.0001$). However, the dispersions obtained with decyl glucoside showed signs of low stability (mainly characterized by signs of creaming) after 2 weeks despite the fact that they were more negatively charged at the time of obtainment. Based on these results, polysorbate 80 at 3% was selected as the aqueous phase surfactant.

Next, the effect of drug incorporation was assessed (**Figure 1 C**). NLC obtained with 5-FU presented smaller diameter than paclitaxel-loaded nanocarriers at both concentrations studied; the most significant difference was in formulations obtained with 1% of drugs and 10% of oil phase (1.33-fold smaller; $p < 0.001$). As all formulations were within the desired size range for the proposed route of administration (200 – 500 nm), NLCs containing 1% of the drugs were selected. Increasing the proportion of the oil phase to 20% reduced particle size by up to 1.26-fold; however, a visual increase in the viscosity of the system was observed, which could make intraductal administration of the formulation difficult. Therefore, NLCs obtained with 10% of oil phase were selected.

Based on these results, optimal formulations were obtained with 1% of cytotoxic drug (paclitaxel or 5-FU), 10% of oil phase (tributyrin and Compritol; 1:1, w/w), 6% of surfactants (Tween 80 and phosphatidylcholine; 1:1, w/w) and 83% of aqueous phase (PBS). From now on, the selected NLC will be referred to as NLC-TB, NLC-TB-P and NLC-TB-5FU, respectively. Their composition is depicted in **Table S2**. Nanocarriers containing tricaprylin as liquid lipid were employed for comparison in cytotoxicity studies, and will be referred to as NLC-TC, NLC-TC-P and NLC-TC-5FU.

The morphological aspects, of the selected nanocarriers (drug-loaded and unloaded) were further assessed using scanning electron microscopy (SEM) and the images revealed the presence of approximately spherical particles with homogeneous distribution and mean sizes in accordance with light scattering findings (**Figure 2**). On day 0, the entrapment efficiencies of paclitaxel and 5-FU in selected NLC-TB dispersed in water were 92.6 ± 0.4% and 60.7 ± 1.5%, respectively, which supports previous observations of higher encapsulation of lipophilic compounds (Andalib, Varshosaz et al. 2012, Bang, Na et al. 2019). NLC freeze-drying promoted a slight reduction on the encapsulation efficiency of paclitaxel and 5-fluorouracil (1.08 and 1.18-fold, respectively).

3.2 Thermal analysis

Thermogravimetric analysis and differential scanning calorimetry were conducted to evaluate the influence of tributyrin (the selected liquid lipid) in Compritol (solid lipid) crystallinity and the influence of drugs on the thermal properties of the lipids. The DSC curve of bulk Compritol shows two endothermic peaks at 73.5 °C and 430.9 °C (**Table 1** and **Figure 3**), which can be associated with the melting point and degradation of the lipid, respectively (Aburahma and Badr-Eldin 2014). Its thermogram presents three main events: first, we observed weight loss due to water evaporation (1.9% of weight loss), followed by a two-step weight loss process (7.0 and 86.7%) related to Compritol degradation with an endothermic peak around 430.9 °C (59.8 J/g), which can be attributed to the molecular complexity of Compritol (mixture of glyceryl mono-, di- and tri-behenates). For tributyrin, three events of weight loss were also observed, which can be attributed to water evaporation or dissociation of other weakly bound molecules, lipid evaporation and degradation (NCBI 2023). The addition of tributyrin slightly reduced the melting temperature of Compritol from 73.5 to 65.9 °C, which was previously attributed in the literature to the molecular interactions between the lipids (Marcial, Carneiro et al. 2017).

In the paclitaxel thermogram, three events were observed: weight loss due to water evaporation (0.6% of weight loss from 25 to 200 °C), paclitaxel fusion (220.5 °C) and exothermic drug degradation (243.6 °C and 47.6 J/g), which is in accordance with previous reports (Marcial, Carneiro et al. 2017). When mixed with Compritol (1:10), the peaks associated to paclitaxel fusion and degradation were not present, suggesting that the drug is incorporated into the lipid matrix in an amorphous state or in a molecularly dispersed state (Yerlikaya, Ozgen et al. 2013, Marcial, Carneiro et al. 2017). In this sample, only two heat flow events were observed, referring to Compritol melting and degradation (73.7 and 430.6

°C, respectively). Similar results were obtained for the mixture of paclitaxel, Compritol and tributyrin (1:5:5). Finally, for 5-fluorouracil, two heat flux events were observed: water loss (0.5% of weight loss from 25 to 120 °C) and drug fusion followed by its degradation (282.2 and 320.9 °C, respectively), which is in accordance with previous reports (Patel, Lakkadwala et al. 2014). When mixed with Compritol, drug thermogravimetric events were not observed, suggesting its amorphization in the lipid matrix (Amasya, Gumustas et al. 2018). However, when tributyrin was added to the mixture, 5-FU decomposition event was observed (282.0 °C), indicating that part of the drug could be in the crystalline state.

The curves obtained for the NLCs suggest a complex system, as evidenced by a change in the curve profiles. The unloaded-NLC (NLC-TB) exhibited a shift in the initial T_{onset} (from 182.8 to 173 °C) compared to the curve of Compritol and tributyrin mixture, suggesting possible interactions between the lipids and the other formulation components in the nanostructured form. No distinct melting points were observed as in the physical mixtures of the components. In drug-loaded NLCs (NLC-TB P and NLC-TB 5FU), a thermal profile similar to unloaded NLC-TB was observed, reinforcing the interaction among the components of the formulation and suggesting that the drug is incorporated in the nanoparticles. Additionally, drug thermogravimetric events (fusion and degradation) were not present, suggesting the amorphization of the drugs in the NLCs (Marcial, Carneiro et al. 2017, Amasya, Gumustas et al. 2018). Interestingly, NLC-TB 5-FU exhibited a weight loss event (3.6%) at 102.4 °C, which was not observed in the other nanocarriers; however, we believe this may be a shift from the weight loss event of the physical mixture of 5-FU, Compritol and tributyrin observed at 145 °C (9.4% of weight loss). Finally, greater stability of the nanocarriers is suggested compared to isolated materials, since their degradation was less abrupt and there was the presence of a greater mass of residue (7.0 – 10.1%) at 500 °C.

3.3 Formulation effects on cell viability

The cytotoxic effects of the nanocarriers were investigated on breast cancer cells as monolayers and spheroids; luminal A (progesterone and estrogen receptors positive) MCF-7 and T-47D cell lines and triple-negative MDA-MB-231 were evaluated (Holliday and Speirs 2011). The experiments were conducted to assess whether (i) paclitaxel or 5-FU incorporation in nanocarriers increased its cytotoxic effects compared to the drug solutions, and (ii) tributyrin incorporation as the liquid lipid increased NLC cytotoxicity. To study selectivity towards tumor cells, non-tumor MCF-10A cells were also treated with selected formulations.

3.3.1 Nanocarriers cytotoxic effects in monolayers

Figure 4 (left panel in A, B, C and D) demonstrates the effects of nanocarriers on cell viability. Nanoparticles obtained using tricaprylin as liquid lipid (NLC-TC) did not reduce cell viability to values below 50%, not even at the highest NLC concentration (50 mg/mL). In turn, nanocarriers obtained with tributyrin (NLC-TB) showed increased cellular cytotoxicity as their concentration increased, resulting in a shift of the viability curve to the left and IC_{50} values ranging between 7.1 and 24.6 mg/mL (**Table 2**). The least pronounced effect was in MDA-MB-231 cells. NLC cytotoxicity was approximately 3-fold greater in MCF-7 and T-47D cells than in the triple negative cancer model, suggesting differences on the cell line sensitivity. As expected, drug incorporation increased the cytotoxicity of NLC-TB.

Comparing the nanocarriers with drug solutions, the cytotoxicity of drug-loaded tributyrin-containing NLC was comparable to the drug solution in tumor cells, resulting in similar values of IC_{50}. On the other hand, higher values of IC_{50} were observed for drug-loaded NLC containing tricaprylin (NLC-TC), both for paclitaxel and 5-fluorouracil. The

IC_{50} of NLC-TB-P was 2 to 6.1-fold lower than NLC-TC-P. For 5-fluorouracil, the differences ranged from 2.3 to 10.8-fold depending on the cell type. For both drugs, the most pronounced differences were observed in MDA-MB-231 cells. Thus, the use of tributyrin as liquid lipid in the nanocarrier brought an advantage in terms of increased cytotoxicity compared to tricaprylin, but not to the drug solution. Due to its higher cytotoxicity, only NLC-TB was evaluated in 3D models.

3.3.2 Nanocarriers cytotoxic effects in 3D models

Three-dimensional culture systems were developed to better mimic the physical and biochemical features of the tumor microenvironment *in vivo* than cell monolayers (Dartora, Salata et al. 2022, Salata and Lopes 2022). MCF-7 and T-47D cells were selected for spheroid production since their spheroids present a compact architecture that facilitates handling and a detailed characterization in the literature (Kapałczyńska, Kolenda et al. 2018). Incorporation of drugs increased nanocarrier cytotoxicity (**Figure 5** and **Table 2**) as expected, resulting in a shift of the viability curve to the left and reduction in IC_{50} values of the formulation. The most pronounced effect was observed for 5-fluorouracil-loaded carriers in T-47D spheroids, in which a 11-fold reduction (from 58.9 mg/mL) was observed on the formulation IC_{50} value when 5-fluorouracil was incorporated.

Comparing the cytotoxicity of drug solutions and drug-loaded NLC-TB, we observed that paclitaxel and 5-FU nanoencapsulation increased their cytotoxicity in MCF-7 spheroids by 2.6- and 3.8-fold compared to their drug solutions, respectively. For T-47D spheroids drug cytotoxicity was increased by 2.0- and 4.0-fold. These results suggest an advantage of the nanocarrier compared to the drug solution in a more representative tumor model.

Images of spheroids were included in **Figure 5** to compare average size and visual aspects before and after treatment. On day 1 after preparation, MCF-7 and T-47D spheroids

presented an approximately spherical morphology and mean sizes of 410.5 ± 14.1 and 365.3 ± 45.4 µm, respectively; on day 5, the size of the spheroids increased by approximately 1.25-fold, and it is possible to see the darker, necrotic center in the images (Dartora, Salata et al. 2022). After treatment with the nanocarriers (at their IC_{50}), the spheroids became darker and a greater presence of loose cells and cellular debris in both cell lines was observed, which is consistent with previous reports (Salata and Lopes 2022). Furthermore, for MCF-7 spheroids, a loosening of cellular packaging and spheroid fragmentation was observed.

3.4 Formulation safety

Although the aim of this study is the local delivery of the incorporated drugs by the intraductal route, it is important to evaluate the safety of the selected formulation in case part of the nanocarriers undergo systemic absorption. The *Galleria mellonella* model was chosen for formulation safety screening before using *in vivo* models since it is easy to handle, provides visible health index results (larvae activity, melanization, survival and pupal formation), is maintained at physiological temperature and allows administration by different routes (in this study, proleg injection was chosen to mimic systemic absorption) (Migotto, Carvalho et al. 2018, Passos, Martino et al. 2020, Piatek, Sheehan et al. 2021). Three days after administration, a significant reduction in the health index of larvae treated with nanocarriers was observed compared to the control (**Figure 6A**), which is consistent with tributyrin ability to increase the NLC cytotoxicity even in the absence of drugs. However, the reduction in health index did not reflect a significant reduction in larval survival (**Figure 6B**), suggesting the overall safety of the formulation for local administration.

3.5 Nanocarriers incorporation in thermosensitive systems

The first step of the NLC incorporation into thermosensitive solutions was the selection of the poloxamer concentration. Solutions containing 1 – 20% of the polymer were prepared and their viscosity under heating was studied using the tube inversion method (Tavakoli, Taymouri et al. 2019). Solutions of poloxamer 11 – 15% were selected for the evaluation of the rheological behavior, as viscosity gain at biological temperature was observed without the formation of a high viscosity gel, which could cause duct obstruction (**Supplementary Table S2**). **Figure 7** and **Supplementary Figure S1** show the rheological behavior and viscosity of selected poloxamer dispersions at 25 and 37°C. Poloxamer aqueous dispersions at 11 – 14% presented linearity between shear stress and shear rate, characterizing a Newtonian fluid behavior (flow index ~ 1, **Supplementary Table S3**). Increasing poloxamer concentration to 15% resulted in absence of linearity between shear stress and shear rate at 37°C and pronounced viscosity gain, characterizing a pseudoplastic behavior (flow index < 1). Poloxamer at 11% was selected because it met the criteria of fluidity at room temperature (which should result in an easy administration) and formation of a fluid gel at physiological temperature for an increased retention in the breast tissue without risking the occurrence of obstruction.

Next, we evaluated whether the rheological behavior of the dispersion was altered upon nanoparticle incorporation. **Figure 7A and B** represents the rheological behavior and viscosity of selected nanocarriers dispersed in water (as obtained), poloxamer aqueous dispersion (at 11%) and NLC dispersed in poloxamer. The NLC dispersed in water exhibited a non-linear relationship between shear stress and shear rate and decrease of viscosity with progressive increases of the shear rate for both temperatures, which is consistent with pseudoplastic rheological behavior (flow indexes of 0.14 and 0.05 at 25 and 37 °C, respectively). In turn, the poloxamer aqueous solution before and after nanocarrier incorporation presented Newtonian rheological behavior at 37°C, represented by the linearity

between shear stress and shear rate. Viscosity gain (1.40- and 2.03-fold for solutions with and without nanocarriers, respectively) at physiological temperature was observed, confirming poloxamer thermoresponsive behavior even after nanoparticle incorporation. Taken together, these results indicate that incorporation of nanoparticles did not alter the rheological and thermosensitive behavior of poloxamer solutions.

3.6. Changes on NLC characteristics and drug encapsulation upon short-term storage

The drug-loaded NLC characteristics were evaluated in a short-term storage study (60 days) and compared to the unloaded formulations. Three experiments were performed to evaluate changes (i) on the NLC as a dispersion (as it was obtained, **Figure 8A**), (ii) on NLC-loaded poloxamer dispersion (**Figure 8B**), and (iii) on the encapsulation efficiency of drugs in the NLC aqueous dispersion as obtained, in the NLC poloxamer dispersion and after freeze-drying (**Figure 8C**). The NLC aqueous dispersions (as obtained) remained stable and within the quality criteria in the first 30 days of the trial. After this period, a significant reduction in the absolute value of the zeta potential and an increase in the diameter of the nanoparticles was observed, especially for drug-loaded NLCs. The diameter of paclitaxel and 5-fluorouracil-loaded nanocarriers increased by 1.3- and 1.7-fold, while the zeta potential decreased by 1.2 and 1.3-fold, respectively. The polydispersity index of the nanoparticles presented more discreet variations over time. No alterations, such as the formation of aggregates or phase separation, were observed macroscopically.

Nanocarriers that were freeze-dried and resuspended in poloxamer dispersion displayed less changes on physicochemical characteristics than the NLC in water (as obtained) during the storage period. After 60 days, less pronounced increases in the mean diameter of unloaded- (1.1-fold), paclitaxel-loaded (1.1-fold) and 5-FU-loaded (1.2-fold) particles were observed compared to initial values compared to the nanocarriers dispersed in

water (**Figure 8B**). No change in the macroscopic aspect of the formulation was observed and there were no pronounced changes in the values of PDI and zeta potential, suggesting that incorporation into the gel improves the stability of the system.

After 30 days of storage, the encapsulation efficiency of the drugs in the NLC aqueous dispersion was reduced (2.3- and 1.8-fold compared to day 0 for paclitaxel and 5-fluorouracil), which may be justified by drug release. As expected, after freeze-drying, the systems preserved drug encapsulation. After 60 days, the encapsulation efficiency of paclitaxel in the NLC aqueous dispersion, NLC poloxamer dispersed in gel and after freeze-drying was 8.65-, 4.11- and 1.08-fold lower. Similar results were obtained for 5-FU: reduction of 6.67-, 2.16 and 1.14-fold in encapsulation efficiencies were observed for NLC dispersed in water, NLC-Poloxamer and freeze-dried samples. These results demonstrate that freeze-drying the NLC can not only enable the obtainment of thermosensitive delivery systems, but also preserve drug encapsulation during short-term storage.

3.7 Evaluation of in vitro drug release

To assess whether NLC incorporation in the poloxamer dispersion prolonged drug release compared to the NLC aqueous dispersion and simple drug solutions, *in vitro* studies were performed. As shown in **Figure 8D**, paclitaxel was released at a slower rate from nanocarriers compared to a drug solution with approximately 53% of the drug released of the NLC by 24 h compared to 94% of drug diffused from the control. Linear correlation coefficient (R^2) values for zero-order, first-order and Higuchi models were 0.9887, 0.7368 and 0.9982, which suggests that drug release kinetics follows the Higuchi model (Marathe, Shadambikar et al. 2022). The incorporation of nanocarriers in gel resulted in a drug release profile similar to its dispersion in water, suggesting that for lipophilic drugs, the main barrier for release is most likely the diffusion out of the lipid matrix. Only at the last time point time

(24 h), drug release from the thermosensitive system differed from the nanocarrier in water, being 1.25-fold smaller. Higher R^2 values were also observed when data was fitted according to the Higuchi model (R^2 = 0.9338).

The release rate of 5-FU from the NLC was faster than paclitaxel, with approximately 33.9 ± 3.4% of the drug being released over the first hour. Smaller amounts of 5-FU were released from the NLC compared to the drug solution within the first hours of the experiment; however, after 8 h no significant difference was observed compared to the control. Data fitting to study release kinetics employed the cumulative drug released until 8 h, since a plateau was observed after this time period. Incorporation in the poloxamer dispersion provided a slower release of 5-fluorouracil: approximately 30% of the drug was released after 8 hours and 44% at the end of the experiment, suggesting the higher impact of the gel matrix for the release of a hydrophilic compound. 5-Fluorouracil release from NLC and the gel containing NLC was best described by the Higuchi model (R^2 = 0.9201 and 0.9583 for NLC dispersion and NLC gel, respectively), which is in accordance with previous studies (Rajinikanth and Chellian 2016).

3.8 Evaluation of Formulation Mammary Tissue Retention

To evaluate the effect of nanocarriers on the retention time in the breast tissue of compounds with different physicochemical properties administered by the intraductal route, we developed nanoparticles with lipo- and hydrophilic fluorescent markers (rhodamine B and Alexa Fluor 647, respectively). Using an *in vivo* imaging system, we compared the retention of markers administered locally or systemically and whether nanocarrier incorporation in the poloxamer solution affected tissue retention. First, nanocarriers without the incorporation of markers were intraductally administered (NLC i.d.) to ensure that the formulation did not show autofluorescence; the absence of tissue autofluorescence was also verified (**Figure 9A**).

Administration of the nanocarrier as aqueous dispersion (as obtained) was more difficult than the fluorophore solution or the poloxamer dispersion, leading to needle obstruction; in three of the animals, about 1/3 less volume was administered compared to the solutions. This was a disadvantage of the NLC dispersion. To account for this technical difficulty, the fluorescence staining along 120 h was measured, and the remaining fluorescence at each time point was calculated to estimate the formulation ability to prolong mammary tissue retention.

Systemic administration of rhodamine-loaded nanocarriers (NLC-R i.p.) resulted in intense fluorescence staining in the abdominal cavity on the day of administration, which was reduced to approximately 18% of the initial intensity after 24h, indicating its distribution and elimination (**Figure 9B**). When compared to systemic administration, intraductally administered rhodamine solution (Sol-R i.d.), rhodamine-loaded NLC (NLC-R i.d.) and its further incorporation in the thermosensitive system (NLC-R Gel i.d.) promoted greater fluorescence signal in the breast tissue, evidencing the advantage of local administration. Staining resulting from the administration of rhodamine-loaded NLC and the solution of the fluorochrome along 120 h was similar, as was the fluorescence decay. In turn, the thermosensitive system resulted in greater permanence of fluorescence staining in the breast tissue: 65.7 ± 18.9% fluorescence intensity was observed on day 5 for the thermosensitive group, compared to 30.7 ± 12.1% and 28.2 ± 10.4% for rhodamine-loaded NLC and rhodamine solution, respectively.

For the hydrophilic marker (Alexa Fluor) a pronounced reduction of fluorescence signal was observed 24 hours after its administration in solution. For NLC dispersed in water, this reduction was less pronounced for up to 48 hours. Reduction of the fluorescence signal in breast tissue was lower when the NLC was incorporated in a thermosensitive system. At the end of the experiment (day 5), we observed that 81.0 ± 11.4%, 37.0 ± 0.0% and 26.6 ± 8.9%

of the fluorescent signal was maintained for the thermosensitive system, lipid carrier and solution, respectively.

To assess local irritation, tissue histology was analyzed after formulations administration (**Figure 10**). Mammary tissue architecture and its typical structures were maintained in all groups, including the cuboidal epithelium of the breast ducts and the surrounding adipocytes and connective tissue (stroma); no inflammatory signs were observed (Masso-Welch, Darcy et al. 2000). Additionally, blood smears were analyzed, which revealed the absence of any changes in numbers or abnormalities in the animals' white blood cell count (**Supplementary Table S4**) (Jacob Filho, Lima et al. 2018). Thus, these results suggest that although addition of tributyrin increased NLC cytotoxicity *in vitro*, it did not lead to changes in blood cell count or local tissue irritation.

4. Discussion

Despite the growing interest, the characteristics and quality attributes of formulations intended for intraductal administration have not been intensively investigated yet (Singh, Gao et al. 2012, Gu, Gao et al. 2018, Joseph, Islam et al. 2020). The ideal nanocarrier diameter to improve drug retention in the ducts, for example, is a matter of debate. Nanoparticles with diameter ranging from a few nanometers to a few micrometers have been investigated, and it seems that, within a specific range, smaller nanoparticles lead to lower tissue retention (Singh, Gao et al. 2012, Gu, Gao et al. 2018, Joseph, Islam et al. 2020). However, an upper limit for nanoparticle diameter that relates to maximal retention without promotion of obstruction (especially in ducts filled with DCIS) is yet to be determined. Avoiding duct obstruction and local damage is important for patients with pre-tumoral lesions and/or for those considering intraductal therapy for prevention (Stearns, Mori et al. 2011). Thus, a size range associated with safety was selected for NLC development here.

Because inclusion of cytotoxic components in nanocarriers has been demonstrated to potentiate drug cytotoxicity, we started this study assessing the possibility to replace the liquid lipid by tributyrin (Migotto, Carvalho et al. 2018, Fukumori, Branco et al. 2023). NLC obtained with tributyrin presented larger particle sizes than those obtained with tricaprylin, which might be related to the viscosity differences and reductions in lipid phase diffusion rates (Eiteman and Goodrum 1994, Jenning, Thünemann et al. 2000). However, cytotoxicity was also reduced with tricaprylin use. NLC obtained with higher surfactant content presented a reduction in nanoparticle size, which can be attributed to the reduction of surface tension, improvement of the stabilization of smaller NLCs and prevention of their coalescence (Gupta, Poudel et al. 2015). The relevance of surfactant type and geometry for NLC characteristics was also observed comparing decyl glucoside (DG) and Tween 80. Despite having have similar HLB values (~15), their molecular geometry is different: while DG has a saturated tail, polysorbate 80 has an unsaturated and kinked chain, which affects the packing of surfactant molecules at the oil-water interface (Saberi, Fang et al. 2013). These differences in packing and steric hindrance effects on the surface of the particles may be associated with the higher stability of polysorbate-based NLCs, despite the relatively lower values of zeta potential compared to decyl glucoside (Li, Qin et al. 2016, Cortés, Hernández-Parra et al. 2021).

An improvement in NLC stability was observed upon nanocarrier incorporation in the poloxamer dispersion (to obtain the *in situ* gel), which is consistent with previous observations by Vaghasiya and colleagues and attributed to the increased viscosity and the three-dimensional network structure of the external phase as temperature increases, prevention of particle aggregation and reduction of polymorphic transitions of the lipid matrix (Vaghasiya, Kumar et al. 2013). Incorporation of NLCs in the poloxamer gel also delayed drug release, which might help to reduce the frequency of administration.

Differences in the release of paclitaxel and 5-FU were observed, with 5-FU release being faster. This is consistent with the higher percentage of non-encapsulated 5-FU in the system (about 40%), which could readily diffuse through the membrane. Additionally, differences in drug solubility might also be involved (Zoubari, Staufenbiel et al. 2017, Mekjaruskul, Beringhs et al. 2021). Zoubari and colleagues demonstrated that the release of lipophilic drugs from lipid carriers occurs more slowly than more hydrophilic drugs (Zoubari, Staufenbiel et al. 2017), which corroborate our observations that paclitaxel was released more slowly than 5-FU.

The inclusion of tributyrin and phosphatidylcholine in the NLC was selected based on the potential advantages of these components for uptake and cytotoxicity. The uptake of NLCs by breast tumor cells has been reported to occur primarily by caveola-mediated endocytosis (Ong, Bañobre-López et al. 2020, Tan, How et al. 2023), but other studies suggest the participation of clathrin in the uptake of lipid nanocarriers by tumor cells (Granja, Nunes et al. 2022). The influence of composition on the uptake of lipid nanoparticles has been demonstrated in previous studies. For example, Zhan and colleagues demonstrated that tumor-derived exosomes in which PC were inserted showed up to a 2-fold increased tumor cell uptake compared to native exosomes (Zhan, Yi et al. 2021). The internalization of phosphatidylcholine and its derivatives seemed to occur preferentially in breast tumor cells compared to normal mammary cells (Villa, Caporizzo et al. 2005). When it comes to cytotoxicity, tributyrin, a pro-drug of butyric acid, demonstrated cytotoxic effects against tumor cells through caspase-3-independent pathways, dissipation of the mitochondrial membrane potential, and epigenetic modulation of histones (Heerdt, Houston et al. 1999, Heidor, Ortega et al. 2012). It increased nanoemulsion cytotoxicity in breast cancer cells even in the absence of drugs (Migotto, Carvalho et al. 2018). Building upon this study, Salata and Lopes demonstrated potentiation of paclitaxel cytotoxicity at a eight-fold lower concentration

(Salata and Lopes 2022). Fukumori *et al.* demonstrated that both tributyrin and tripropionin increased the cytotoxicity of 5-FU in multiple nanoemulsion, but the magnitude of this effect depended on the mutation status of colorectal cancer cells (Fukumori, Branco et al. 2023). Bras-Gonçalves and colleagues also demonstrated the ability of a butyrate derivative (3-n-butyrate) to increase the effectiveness of 5-FU in colorectal cancer cells (Bras-Gonçalves, Pocard et al. 2001). Although we did not study the impact of PC for nanocarrier internalization here, our results corroborate the ability of tributyrin to improve the cytotoxicity of NLC despite the differences in the physical state of the nanocarriers: the NLC is solid at body temperature while nanoemulsions (employed in previous studies) are liquid. The increase in cytotoxicity upon the replacement of tricaprylin by tributyrin was more pronounced with the unloaded NLC. Nevertheless, even though drug release was slower from the nanocarrier compared to the solution, IC_{50} values for drug-loaded NLC-TB and drug solutions were closer (and lower) than for NLC-TC. These results demonstrate the relevance of optimizing NLC production to enable tributyrin use. Additionally, the cytotoxicity increase of the drug-loaded NLC due to tributyrin incorporation was more pronounced in MDA-MB-231 cells, which is interesting considering that there are limited options for triple negative breast cancer treatment.

Another interesting finding was that nanoencapsulation promoted a more pronounced reduction in the IC_{50} of drugs in spheroids than in cell monolayers. Differences in viability upon exposure to free or nanoencapsulated drugs have been reported for spheroids from several cell lines (Juarez-Moreno, Chavez-Garcia et al. 2022). Since the three-dimensional cell culture model better mimics drug diffusion characteristics and hurdles observed *in vivo*, it is reasonable to suggest that nanoparticles might contribute to improve drug penetration into the inner core of the spheroid as observed for other nanocarriers (Dartora, Salata et al. 2022),

leading to increased drug accumulation and a more pronounced cytotoxic effect in spheroids (Grabowska-Jadach, Zuchowska et al. 2018, Juarez-Moreno, Chavez-Garcia et al. 2022).

Nanocarrier modification with bioadhesive components and the administration of gels have been demonstrated to prolong local retention of drugs (Joseph, Islam et al. 2020, Dartora, Salata et al. 2022, Salata and Lopes 2022), which is relevant for reduction of the frequency of administration, especially if we consider the technical difficulties described for the intraductal administration (Love, Zhang et al. 2013). This led us to investigate the association of NLC and an *in situ* poloxamer-based gel for prolongation of mammary retention. Our results support the relevance of this association. Despite the difficulties in the administration of the NLC aqueous dispersion (which constitute a disadvantage of the nanocarrier), it was able to prolong the mammary retention of the hydrophilic, but not the hydrophobic, fluorophore. On the other hand, incorporation of the nanocarrier in the poloxamer dispersion seemed to prolong both. The lipophilicity of incorporated compounds has been demonstrated to influence the ability of nanocarriers to prolong their retention in the mammary tissue. For example, more lipophilic drugs are more likely to remain longer in the ducts and mammary tissue because of interactions with fat components independently of their encapsulation (Sapienza Passos, Dartora et al. 2023). This justifies doxorubicin hydrochloride enhanced tissue permanence ($t_{1/2}$ of 2.0 ± 0.4 h, solubility in water ~50 mg/mL) compared to fluorescein disodium (14.5 min, solubility in water ~500 mg/mL) (Singh, Gao et al. 2012). We have previously observed that a nanoemulsion affected more pronouncedly the retention of the hydrophilic Alexa fluor compared to the lipophilic C6 ceramide (Migotto, Carvalho et al. 2018, Carvalho, Salata et al. 2019). Therefore, in addition to aiding stability, addition of nanoparticles into the poloxamer matrix seemed to prolong mammary retention. This effect might be attributed to the aggregation of the hydrophobic blocks of the polymer and gel formation with increasing temperature, reducing tissue clearance of encapsulated compounds

(Ci, Huang et al. 2017, Soliman, Ullah et al. 2019). Increases in tissue retention allows a reduction in dose frequency, and might contribute to treatment adherence and efficacy (Shaker, Shaker et al. 2016).

5. Conclusion

In this study, we optimized nanostructured lipid carriers for the intraductal administration of paclitaxel and 5-fluorouracil. The selection of tributyrin as oil phase was essential to increase cytotoxicity in tumor cells, but to use phosphatidylcholine as a surfactant and tributyrin as the liquid lipid, longer sonication times were required to achieve the desired nanocarrier size. Incorporation of selected nanoparticles into poloxamer thermosensitive gels contributed to the (i) sustained drug release and improved stability upon short-term storage of the NLC, and (ii) prolonged *in vivo* retention of fluorescent markers with distinct physicochemical characteristics. Taken together, the results from this study contribute to improving our understanding of nanocarrier design with increased cytotoxicity and prolonged retention for the intraductal route and local breast cancer treatment.

Acknowledgements

The authors acknowledge the technical assistance of Mr. Moacir de Britto. This study was funded by FAPESP, grant# 2018/13877-1, #2019/08582-5, #2020/01208-8), CNPq (grant #306866/2020-0) and CAPES – Brazilian Federal Agency for Support and Evaluation of Graduate Education within the Ministry of Education of Brazil (finance code 001). This study is part of the National Institute of Science and Technology in Pharmaceutical Nanotechnology: a transdisciplinary approach INCT-NANOFARMA, which is supported by FAPESP (grant #2014/50928-2) and CNPq (grant # 465687/2014-8).

AUTHOR CONTRIBUTIONS

Julia S. Passos: Conceptualization, Methodology, Validation, Formal analysis, Investigation, Writing – Original draft, Writing – review & editing. **Alexsandra C. Apolinario:** Conceptualization, Methodology, Writing – review & editing. **Kelly Ishida:** Conceptualization, Validation, Resources, Writing – review & editing, Supervision. **Tereza S. Martins:** Methodology, Validation, Formal analysis, Investigation, Writing – review & editing. **Luciana B. Lopes:** Conceptualization, Methodology, Validation, Formal analysis, Investigation, Writing – Original draft, Writing – review & editing, Resources, Supervision, Project administration, Funding acquisition.

REFERENCES

Aburahma, M. H. and S. M. Badr-Eldin (2014). "Compritol 888 ATO: a multifunctional lipid excipient in drug delivery systems and nanopharmaceuticals." Expert Opin Drug Deliv **11**(12): 1865-1883.

Amasya, G., M. Gumustas, U. Badilli, S. A. Ozkan and N. Tarimci (2018). "Development of a HILIC method for the determination of 5-fluorouracil from nano drug delivery systems and rat skin extracts." J Pharm Biomed Anal **154**: 285-293.

Andalib, S., J. Varshosaz, F. Hassanzadeh and H. Sadeghi (2012). "Optimization of LDL targeted nanostructured lipid carriers of 5-FU by a full factorial design." Adv Biomed Res **1**: 45.

Apolinário, A. C., G. C. Salata, M. M. de Souza, M. Chorilli and L. B. Lopes (2022). "Rethinking Breast Cancer Chemoprevention: Technological Advantages and Enhanced Performance of a Nanoethosomal-Based Hydrogel for Topical Administration of Fenretinide." AAPS PharmSciTech **23**(4): 104.

Badve, S. S. and Y. Gökmen-Polar (2019). "Ductal carcinoma in situ of breast: update 2019." Pathology **51**(6): 563-569.

Bang, K. H., Y. G. Na, H. W. Huh, S. J. Hwang, M. S. Kim, M. Kim, H. K. Lee and C. W. Cho (2019). "The Delivery Strategy of Paclitaxel Nanostructured Lipid Carrier Coated with Platelet Membrane." Cancers (Basel) **11**(6).

Barnes, H. A. H., J. F. Walters, K. (1989). An Introduction to Rheology.

Bernabeu, E., M. Cagel, E. Lagomarsino, M. Moretton and D. A. Chiappetta (2017). "Paclitaxel: What has been done and the challenges remain ahead." Int J Pharm **526**(1-2): 474-495.

Bras-Gonçalves, R. A., M. Pocard, J. L. Formento, F. Poirson-Bichat, G. De Pinieux, I. Pandrea, F. Arvelo, G. Ronco, P. Villa, A. Coquelle, G. Milano, T. Lesuffleur, B. Dutrillaux and M. F. Poupon (2001). "Synergistic efficacy of 3n-butyrate and 5-fluorouracil in human colorectal cancer xenografts via modulation of DNA synthesis." Gastroenterology **120**(4): 874-888.

Carvalho, V. F. M., A. Migotto, D. V. Giacone, D. P. de Lemos, T. B. Zanoni, S. S. Maria-Engler, L. V. Costa-Lotufo and L. B. Lopes (2017). "Co-encapsulation of paclitaxel and C6 ceramide in tributyrin-containing nanocarriers improve co-localization in the skin and potentiate cytotoxic effects in 2D and 3D models." Eur J Pharm Sci **109**: 131-143.

Carvalho, V. F. M., G. C. Salata, J. K. R. de Matos, S. Costa-Fernandez, M. Chorilli, A. A. Steiner, G. L. B. de Araujo, E. R. Silveira, L. V. Costa-Lotufo and L. B. Lopes (2019). "Optimization of composition and obtainment parameters of biocompatible nanoemulsions intended for intraductal administration of piplartine (piperlongumine) and mammary tissue targeting." Int J Pharm **567**: 118460.

Chand, P., H. Kumar, N. Badduri, N. V. Gupta, V. G. Bettada, S. V. Madhunapantula, S. S. Kesharwani, S. Dey and V. Jain (2021). "Design and evaluation of cabazitaxel loaded NLCs against breast cancer cell lines." Colloids Surf B Biointerfaces **199**: 111535.

Chun, Y. S., S. Bisht, V. Chenna, D. Pramanik, T. Yoshida, S. M. Hong, R. F. de Wilde, Z. Zhang, D. L. Huso, M. Zhao, M. A. Rudek, V. Stearns, A. Maitra and S. Sukumar (2012). "Intraductal administration of a polymeric nanoparticle formulation of curcumin (NanoCurc) significantly attenuates incidence of mammary tumors in a rodent chemical carcinogenesis model: Implications for breast cancer chemoprevention in at-risk populations." Carcinogenesis **33**(11): 2242-2249.

Ci, L., Z. Huang, Y. Liu, Z. Liu, G. Wei and W. Lu (2017). "Amino-functionalized poloxamer 407 with both mucoadhesive and thermosensitive properties: preparation, characterization and application in a vaginal drug delivery system." Acta Pharm Sin B **7**(5): 593-602.

Cortés, H., H. Hernández-Parra, S. A. Bernal-Chávez, M. L. D. Prado-Audelo, I. H. Caballero-Florán, F. V. Borbolla-Jiménez, M. González-Torres, J. J. Magaña and G. Leyva-Gómez (2021). "Non-Ionic Surfactants for Stabilization of Polymeric Nanoparticles for Biomedical Uses." Materials (Basel) **14**(12).

Costa, P. and J. M. S. Lobo (2001). "Modeling and comparison of dissolution profiles." European Journal of Pharmaceutical Sciences **13**(2): 123-133.

Danaei, M., M. Dehghankhold, S. Ataei, F. Hasanzadeh Davarani, R. Javanmard, A. Dokhani, S. Khorasani and M. R. Mozafari (2018). "Impact of Particle Size and Polydispersity Index on the Clinical Applications of Lipidic Nanocarrier Systems." Pharmaceutics **10**(2).

Dartora, V. F. C., G. C. Salata, J. S. Passos, P. C. Branco, E. Silveira, A. A. Steiner, L. V. Costa-Lotufo and L. B. Lopes (2022). "Hyaluronic acid nanoemulsions improve piplartine cytotoxicity in 2D and 3D breast cancer models and reduce tumor development after intraductal administration." Int J Biol Macromol.

Del Mastro, L., F. Poggio, E. Blondeaux, S. De Placido, M. Giuliano, V. Forestieri, M. De Laurentiis, A. Gravina, G. Bisagni, A. Rimanti, A. Turletti, C. Nisticò, A. Vaccaro, F. Cognetti, A. Fabi, S. Gasparro, O. Garrone, M. G. Alicicco, Y. Urracci, M. Mansutti, P. Poletti, P. Correale, C. Bighin, F. Puglisi, F. Montemurro, G. Colantuoni, M. Lambertini, L. Boni, M. Venturini, A. Abate, S. Pastorino, G. Canavese, C. Vecchio, M. Guenzi, M. Lambertini, A. Levaggi, S. Giraudi, V. Accortanzo, C. A. Floris, E. Aitini, G. Fornari, S. Miraglia, G. Buonfanti, M. C. Cherchi, F. Petrelli, A. Vaccaro, E. Magnolfi, A. Contu, R. Labianca, A. Parisi, C. Basurto, F. Cappuzzo, M. Merlano, S. Russo, M. Mansutti, E. Poletto, M. Nardi, D. Grasso, A. Fontana, L. Isa, M. Comandè, L. Cavanna, S. Iacobelli, S. Milani, G. Mustacchi, S. Venturini, A. F. Scinto, M. G. Sarobba, P. Pugliese, A. Bernardo, I. Pavese, M. Coccaro, B. Massidda, M. T. Ionta, A. Nuzzo, L. Laudadio, V. Chiantera, R. Dottori, M. Barduagni, F. Castiglione, F. Ciardiello, V. Tinessa, A. Ficorella, L. Moscetti, I. Vallini, G. Giardina, R. Silva, M. Montedoro, E. Seles, F. Morano, G. Cruciani, V. Adamo, A. Pancotti, V. Palmisani, A. Ruggeri, E. Cammilluzzi, F. Carrozza, M. D'Aprile, M. Brunetti, P. Gallotti, E. Chiesa, F. Testore, A. D'Arco, A. Ferro, A. Jirillo, M. Pezzoli, G. Scambia, C. Iacono, P. Masullo, G. Tomasello, G. Gandini, A. Zoboli, C. Bottero, M. Cazzaniga, G. Genua, S. Palazzo, M. D'Amico and D. Perrone (2022). "Fluorouracil and dose-dense adjuvant chemotherapy in patients with early-stage breast cancer (GIM2): end-of-study results from a randomised, phase 3 trial." The Lancet Oncology **23**(12): 1571-1582.

Dewan, M., B. Bhowmick, G. Sarkar, D. Rana, M. K. Bain, M. Bhowmik and D. Chattopadhyay (2015). "Effect of methyl cellulose on gelation behavior and drug release from poloxamer based ophthalmic formulations." Int J Biol Macromol **72**: 706-710.

Eiteman, M. A. and J. W. Goodrum (1994). "Density and viscosity of low-molecular weight triglycerides and their mixtures." Journal of the American Oil Chemists' Society **71**: 1261–1265.
Fujii, T., F. Le Du, L. Xiao, T. Kogawa, C. H. Barcenas, R. H. Alvarez, V. Valero, Y. Shen and N. T. Ueno (2015). "Effectiveness of an Adjuvant Chemotherapy Regimen for Early-Stage Breast Cancer: A Systematic Review and Network Meta-analysis." JAMA Oncol **1**(9): 1311-1318.
Fukumori, C., P. C. Branco, T. Barreto, K. Ishida and L. B. Lopes (2023). "Development and cytotoxicity evaluation of multiple nanoemulsions for oral co-delivery of 5-fluorouracil and short chain triglycerides for colorectal cancer." Eur J Pharm Sci **187**: 106465.
Gadag, S., R. Narayan, A. S. Nayak, D. Catalina Ardila, S. Sant, Y. Nayak, S. Garg and U. Y. Nayak (2021). "Development and preclinical evaluation of microneedle-assisted resveratrol loaded nanostructured lipid carriers for localized delivery to breast cancer therapy." Int J Pharm **606**: 120877.
Gao, D., J. Liu, J. Yuan, J. Wu, X. Kuang, D. Kong, W. Zheng, G. Wang, S. Sukumar, Y. Tu, C. Chen and S. Sun (2021). "Intraductal administration of N-methyl-N-nitrosourea as a novel rodent mammary tumor model." Ann Transl Med **9**(7): 576.
Garg, N. K., N. Tandel, S. K. Bhadada and R. K. Tyagi (2021). "Nanostructured Lipid Carrier-Mediated Transdermal Delivery of Aceclofenac Hydrogel Present an Effective Therapeutic Approach for Inflammatory Diseases." Front Pharmacol **12**: 713616.
Grabowska-Jadach, I., A. Zuchowska, M. Olesik, M. Drozd, M. Pietrzak, E. Malinowska and Z. Brzozkaa (2018). "Cytotoxicity studies of selected cadmium-based quantum dots on 2D vs. 3D cell cultures." New Journal of Chemistry **42**(15): 12787-12795.
Gradishar, W. J. (2006). "Albumin-bound paclitaxel: a next-generation taxane." Expert Opin Pharmacother **7**(8): 1041-1053.
Granja, A., C. Nunes, C. T. Sousa and S. Reis (2022). "Folate receptor-mediated delivery of mitoxantrone-loaded solid lipid nanoparticles to breast cancer cells." Biomedicine & Pharmacotherapy **154**: 113525.
Groen, E. J., L. E. Elshof, L. L. Visser, E. J. T. Rutgers, H. A. O. Winter-Warnars, E. H. Lips and J. Wesseling (2017). "Finding the balance between over- and under-treatment of ductal carcinoma in situ (DCIS)." Breast **31**: 274-283.
Gu, Z., D. Gao, F. Al-Zubaydi, S. Li, Y. Singh, K. Rivera, J. Holloway, Z. Szekely, S. Love and P. J. Sinko (2018). "The effect of size and polymer architecture of doxorubicin-poly(ethylene) glycol conjugate nanocarriers on breast duct retention, potency and toxicity." Eur J Pharm Sci **121**: 118-125.
Gupta, B., B. K. Poudel, T. H. Tran, R. Pradhan, H. J. Cho, J. H. Jeong, B. S. Shin, H. G. Choi, C. S. Yong and J. O. Kim (2015). "Modulation of Pharmacokinetic and Cytotoxicity Profile of Imatinib Base by Employing Optimized Nanostructured Lipid Carriers." Pharm Res **32**(9): 2912-2927.
Hanif, M., M. F. Akhtar, S. Naeem, M. Wahid, M. A. Shehzad, M. Saadullah, B. Nasir and S. Afzal (2018). "Development and Validation of a New HPLC Method For the Detection of 5-Fluorouracil in Mobile Phase and in Plasma." Current Pharmaceutical Analysis **14**(1): 3 - 7.
Heerdt, B. G., M. A. Houston, G. M. Anthony and L. H. Augenlicht (1999). "Initiation of growth arrest and apoptosis of MCF-7 mammary carcinoma cells by tributyrin, a triglyceride analogue of the short-chain fatty acid butyrate, is associated with mitochondrial activity." Cancer Res **59**(7): 1584-1591.
Heidor, R., J. F. Ortega, A. de Conti, T. P. Ong and F. S. Moreno (2012). "Anticarcinogenic actions of tributyrin, a butyric acid prodrug." Curr Drug Targets **13**(14): 1720-1729.
Holliday, D. L. and V. Speirs (2011). "Choosing the right cell line for breast cancer research." Breast Cancer Res **13**(4): 215.
Hosmer, J. M., S. H. Shin, A. Nornoo, H. Zheng and L. B. Lopes (2011). "Influence of internal structure and composition of liquid crystalline phases on topical delivery of paclitaxel." J Pharm Sci **100**(4): 1444-1455.
Hosmer, J. M., A. A. Steiner and L. B. Lopes (2013). "Lamellar liquid crystalline phases for cutaneous delivery of Paclitaxel: impact of the monoglyceride." Pharm Res **30**(3): 694-706.

Jacob Filho, W., C. C. Lima, M. R. R. Paunksnis, A. A. Silva, M. S. Perilhão, M. Caldeira, D. Bocalini and R. R. de Souza (2018). "Reference database of hematological parameters for growing and aging rats." Aging Male **21**(2): 145-148.

Jain, A. and S. K. Jain (2016). "IN VITRO RELEASE KINETICS MODEL FITTING OF LIPOSOMES: AN INSIGHT." Chem Phys Lipids.

Jain, S., D. Kumar, N. K. Swarnakar and K. Thanki (2012). "Polyelectrolyte stabilized multilayered liposomes for oral delivery of paclitaxel." Biomaterials **33**(28): 6758-6768.

Jenning, V., A. F. Thünemann and S. H. Gohla (2000). "Characterisation of a novel solid lipid nanoparticle carrier system based on binary mixtures of liquid and solid lipids." Int J Pharm **199**(2): 167-177.

Joseph, M. K., M. Islam, J. Reineke, M. Hildreth, T. Woyengo, A. Pillatzki, A. Baride and O. Perumal (2020). "Intraductal Drug Delivery to the Breast: Effect of Particle Size and Formulation on Breast Duct and Lymph Node Retention." Mol Pharm **17**(2): 441-452.

Juarez-Moreno, K., D. Chavez-Garcia, G. Hirata and R. Vazquez-Duhalt (2022). "Monolayer (2D) or spheroids (3D) cell cultures for nanotoxicological studies? Comparison of cytotoxicity and cell internalization of nanoparticles." Toxicol In Vitro **85**: 105461.

Kapałczyńska, M., T. Kolenda, W. Przybyła, M. Zajączkowska, A. Teresiak, V. Filas, M. Ibbs, R. Bliźniak, Ł. Łuczewski and K. Lamperska (2018). "2D and 3D cell cultures - a comparison of different types of cancer cell cultures." Arch Med Sci **14**(4): 910-919.

Karakash, I., J. Vasileska, D. Shalabalija, L. Mihailova, M. G. Dodov, R. S. Raicki and M. S. Crcarevska (2020). Freeze-drying of nanostructured lipid carriers loaded with Salvia off. extract for Alzheimer's disease treatment Macedonian Pharmaceutical Bulletin. **66:** 219-220.

Khan, A. A., J. Mudassir, S. Akhtar, V. Murugaiyah and Y. Darwis (2019). "Freeze-Dried Lopinavir-Loaded Nanostructured Lipid Carriers for Enhanced Cellular Uptake and Bioavailability: Statistical Optimization, in Vitro and in Vivo Evaluations." Pharmaceutics **11**(2).

Korde, L. A., M. R. Somerfield, L. A. Carey, J. R. Crews, N. Denduluri, E. S. Hwang, S. A. Khan, S. Loibl, E. A. Morris, A. Perez, M. M. Regan, P. A. Spears, P. K. Sudheendra, W. F. Symmans, R. L. Yung, B. E. Harvey and D. L. Hershman (2021). "Neoadjuvant Chemotherapy, Endocrine Therapy, and Targeted Therapy for Breast Cancer: ASCO Guideline." J Clin Oncol **39**(13): 1485-1505.

Kuang, X. W., J. H. Liu, Z. H. Sun, S. Sukumar, S. R. Sun and C. Chen (2020). "Intraductal Therapy in Breast Cancer: Current Status and Future Prospective." J Mammary Gland Biol Neoplasia **25**(2): 133-143.

Lanna, E. G., R. P. Siqueira, M. G. C. Machado, A. de Souza, I. C. Trindade, R. T. Branquinho and V. C. F. Mosqueira (2021). "Lipid-based nanocarriers co-loaded with artemether and triglycerides of docosahexaenoic acid: Effects on human breast cancer cells." Biomed Pharmacother **134**: 111114.

Li, X., Y. Qin, C. Liu, S. Jiang, L. Xiong and Q. Sun (2016). "Size-controlled starch nanoparticles prepared by self-assembly with different green surfactant: The effect of electrostatic repulsion or steric hindrance." Food Chem **199**: 356-363.

Longley, D. B., D. P. Harkin and P. G. Johnston (2003). "5-fluorouracil: mechanisms of action and clinical strategies." Nat Rev Cancer **3**(5): 330-338.

Losito, D. W., P. S. Lopes, A. R. Ueoka, M. C. A. Fantini, P. L. Oseliero Filho, N. Andréo-Filho and T. S. Martins (2021). Biocomposites based on SBA-15 and papain: Characterization, enzymatic activity and cytotoxicity evaluation. Microporous and Mesoporous Materials, Elsevier. **325:** 111316.

Love, S. M., W. Zhang, E. J. Gordon, J. Rao, H. Yang, J. Li, B. Zhang, X. Wang, G. Chen and B. Zhang (2013). "A feasibility study of the intraductal administration of chemotherapy." Cancer Prev Res (Phila) **6**(1): 51-58.

Mahoney, M. E., E. J. Gordon, J. Y. Rao, Y. Jin, N. Hylton and S. M. Love (2013). "Intraductal therapy of ductal carcinoma in situ: a presurgery study." Clin Breast Cancer **13**(4): 280-286.

Marathe, S., G. Shadambikar, T. Mehraj, S. P. Sulochana, N. Dudhipala and S. Majumdar (2022). "Development of α-Tocopherol Succinate-Based Nanostructured Lipid Carriers for Delivery of Paclitaxel." Pharmaceutics **14**(5).
Marcial, S. P. d. S., G. Carneiro and E. A. Leite (2017). "Lipid-based nanoparticles as drug delivery system for paclitaxel in breast cancer treatment." Journal of Nanoparticle Research **19**(340).
Marupudi, N. I., J. E. Han, K. W. Li, V. M. Renard, B. M. Tyler and H. Brem (2007). "Paclitaxel: a review of adverse toxicities and novel delivery strategies." Expert Opin Drug Saf **6**(5): 609-621.
Masso-Welch, P. A., K. M. Darcy, N. C. Stangle-Castor and M. M. Ip (2000). "A developmental atlas of rat mammary gland histology." J Mammary Gland Biol Neoplasia **5**(2): 165-185.
Mekjaruskul, C., A. O. Beringhs, W. C. Luo, Q. Xu, M. Halquist, B. Qin, Y. Wang and X. Lu (2021). "Impact of Membranes on In Vitro Release Assessment: a Case Study Using Dexamethasone." AAPS PharmSciTech **22**(1): 42.
Migotto, A., V. F. M. Carvalho, G. C. Salata, F. W. M. da Silva, C. Y. I. Yan, K. Ishida, L. V. Costa-Lotufo, A. A. Steiner and L. B. Lopes (2018). "Multifunctional nanoemulsions for intraductal delivery as a new platform for local treatment of breast cancer." Drug Deliv **25**(1): 654-667.
Moo, T.-A., R. Sanford, C. Dang and M. Morrow (2018). "Overview of Breast Cancer Therapy." PET Clinics **13**(3): 339-354.
Murata, S., S. L. Kominsky, M. Vali, Z. Zhang, E. Garrett-Mayer, D. Korz, D. Huso, S. D. Baker, J. Barber, E. Jaffee, R. T. Reilly and S. Sukumar (2006). "Ductal access for prevention and therapy of mammary tumors." Cancer Res **66**(2): 638-645.
Narod, S. A., J. Iqbal, V. Giannakeas, V. Sopik and P. Sun (2015). "Breast Cancer Mortality After a Diagnosis of Ductal Carcinoma In Situ." JAMA Oncol **1**(7): 888-896.
NCBI (2021). 5-Fluorouracil. PubChem CID 3385.
NCBI (2022). Paclitaxel. PubChem CID 36314.
NCBI (2023). Tributyrin. PubChem CID 6050.
Okugawa, H., D. Yamamoto, Y. Uemura, N. Sakaida, A. Tanano, K. Tanaka and Y. Kamiyama (2005). "Effect of perductal paclitaxel exposure on the development of MNU-induced mammary carcinoma in female S-D rats." Breast Cancer Res Treat **91**(1): 29-34.
Ong, Y. S., M. Bañobre-López, S. A. C. Lima and S. Reis (2020). "A multifunctional nanomedicine platform for co-delivery of methotrexate and mild hyperthermia towards breast cancer therapy." Materials Science and Engineering: C **116**: 111255.
Passos, J. S., L. C. Martino, V. F. C. Dartora, G. L. B. Araujo, K. Ishida and L. B. Lopes (2020). "Development, skin targeting and antifungal efficacy of topical lipid nanoparticles containing itraconazole." Eur J Pharm Sci **149**: 105296.
Patel, M. N., S. Lakkadwala, M. S. Majrad, E. R. Injeti, S. M. Gollmer, Z. A. Shah, S. H. Boddu and J. Nesamony (2014). "Characterization and evaluation of 5-fluorouracil-loaded solid lipid nanoparticles prepared via a temperature-modulated solidification technique." AAPS PharmSciTech **15**(6): 1498-1508.
Patil, A., R. Narvenker, B. Prabhakar and P. Shende (2020). "Strategic consideration for effective chemotherapeutic transportation via transpapillary route in breast cancer." Int J Pharm **586**: 119563.
Pedro, I. D. R., O. P. Almeida, H. R. Martins, J. de Alcântara Lemos, A. L. B. de Barros, E. A. Leite and G. Carneiro (2019). "Optimization and in vitro/in vivo performance of paclitaxel-loaded nanostructured lipid carriers for breast cancer treatment." Journal of Drug Delivery Science and Technology **54**: 101370.
Piatek, M., G. Sheehan and K. Kavanagh (2021). ": The Versatile Host for Drug Discovery, In Vivo Toxicity Testing and Characterising Host-Pathogen Interactions." Antibiotics (Basel) **10**(12).
Poonia, N., J. Kaur Narang, V. Lather, S. Beg, T. Sharma, B. Singh and D. Pandita (2019). "Resveratrol loaded functionalized nanostructured lipid carriers for breast cancer targeting:

Systematic development, characterization and pharmacokinetic evaluation." Colloids Surf B Biointerfaces **181**: 756-766.
Rajinikanth, P. S. and J. Chellian (2016). "Development and evaluation of nanostructured lipid carrier-based hydrogel for topical delivery of 5-fluorouracil." Int J Nanomedicine **11**: 5067-5077.
Saberi, A. H., Y. Fang and D. J. McClements (2013). "Fabrication of vitamin E-enriched nanoemulsions: factors affecting particle size using spontaneous emulsification." J Colloid Interface Sci **391**: 95-102.
Sagara, Y., W. Julia, M. Golshan and M. Toi (2017). "Paradigm Shift toward Reducing Overtreatment of Ductal Carcinoma." Front Oncol **7**: 192.
Salata, G. C. and L. B. Lopes (2022). "Phosphatidylcholine-Based Nanoemulsions for Paclitaxel and a P-Glycoprotein Inhibitor Delivery and Breast Cancer Intraductal Treatment." Pharmaceuticals (Basel) **15**(9).
Salata, G. C., I. D. Malagó, V. F. M. Carvalho Dartora, A. F. Marçal Pessoa, M. C. A. Fantini, S. K. P. Costa, J. A. Machado-Neto and L. B. Lopes (2021). "Microemulsion for Prolonged Release of Fenretinide in the Mammary Tissue and Prevention of Breast Cancer Development." Mol Pharm **18**(9): 3401-3417.
Sapienza Passos, J., V. Dartora, G. Cassone Salata, I. Draszesski Malagó and L. B. Lopes (2023). "Contributions of nanotechnology to the intraductal drug delivery for local treatment and prevention of breast cancer." Int J Pharm **635**: 122681.
Shaker, D. S., M. A. Shaker, A. Klingner and M. S. Hanafy (2016). "In situ thermosensitive Tamoxifen citrate loaded hydrogels: An effective tool in breast cancer loco-regional therapy." Journal of Drug Delivery Science and Technology **35**: 155-164.
Shamma, R. N. and M. H. Aburahma (2014). "Follicular delivery of spironolactone via nanostructured lipid carriers for management of alopecia." International journal of nanomedicine **9**: 5449-5460.
Singh, Y., D. Gao, Z. Gu, S. Li, K. A. Rivera, S. Stein, S. Love and P. J. Sinko (2012). "Influence of molecular size on the retention of polymeric nanocarrier diagnostic agents in breast ducts." Pharm Res **29**(9): 2377-2388.
Sinko, P. J. (2011). Rheology. Martin's physical pharmacy and pharmaceutical sciences: physical chemical and biopharmaceutical principles in the pharmaceutical sciences. P. J. Sinko**:** 469-491.
Soliman, K. A., K. Ullah, A. Shah, D. S. Jones and T. R. R. Singh (2019). "Poloxamer-based in situ gelling thermoresponsive systems for ocular drug delivery applications." Drug Discov Today **24**(8): 1575-1586.
Stearns, V., T. Mori, L. K. Jacobs, N. F. Khouri, E. Gabrielson, T. Yoshida, S. L. Kominsky, D. L. Huso, S. Jeter, P. Powers, K. Tarpinian, R. J. Brown, J. R. Lange, M. A. Rudek, Z. Zhang, T. N. Tsangaris and S. Sukumar (2011). "Preclinical and clinical evaluation of intraductally administered agents in early breast cancer." Sci Transl Med **3**(106): 106ra108.
Tan, L. K. S., C. W. How, L. E. Low, B. H. Ong, J. S. Loh, S.-Y. Lim, Y. S. Ong and J. B. Foo (2023). "Magnetic-guided targeted delivery of zerumbone/SPION co-loaded in nanostructured lipid carrier into breast cancer cells." Journal of Drug Delivery Science and Technology **87**: 104830.
Tavakoli, N., S. Taymouri, A. Saeidi and V. Akbari (2019). "Thermosensitive hydrogel containing sertaconazole loaded nanostructured lipid carriers for potential treatment of fungal keratitis." Pharm Dev Technol **24**(7): 891-901.
Vaghasiya, H., A. Kumar and K. Sawant (2013). "Development of solid lipid nanoparticles based controlled release system for topical delivery of terbinafine hydrochloride." Eur J Pharm Sci **49**(2): 311-322.
van Seijen, M., E. H. Lips, A. M. Thompson, S. Nik-Zainal, A. Futreal, E. S. Hwang, E. Verschuur, J. Lane, J. Jonkers, D. W. Rea, J. Wesseling and P. team (2019). "Ductal carcinoma in situ: to treat or not to treat, that is the question." Br J Cancer **121**(4): 285-292.
Vater, C., A. Apanovic, C. Riethmüller, B. Litschauer, M. Wolzt, C. Valenta and V. Klang (2021). "Changes in Skin Barrier Function after Repeated Exposition to Phospholipid-Based

Surfactants and Sodium Dodecyl Sulfate In Vivo and Corneocyte Surface Analysis by Atomic Force Microscopy." Pharmaceutics **13**(4).
Villa, A. M., E. Caporizzo, A. Papagni, L. Miozzo, P. Del Buttero, M. D. Grilli, N. Amboldi, F. Fazio, S. M. Doglia and B. Giglioni (2005). "Choline and phosphatidylcholine fluorescent derivatives localization in carcinoma cells studied by laser scanning confocal fluorescence microscopy." Eur J Cancer **41**(10): 1453-1459.
Weaver, B. A. (2014). "How Taxol/paclitaxel kills cancer cells." Mol Biol Cell **25**(18): 2677-2681.
Wünsch, A., D. Mulac and K. Langer (2021). "Lecithin coating as universal stabilization and functionalization strategy for nanosized drug carriers to overcome the blood-brain barrier." Int J Pharm **593**: 120146.
Yerlikaya, F., A. Ozgen, I. Vural, O. Guven, E. Karaagaoglu, M. A. Khan and Y. Capan (2013). "Development and evaluation of paclitaxel nanoparticles using a quality-by-design approach." J Pharm Sci **102**(10): 3748-3761.
Yoon, H. Y., I. H. Chang, Y. T. Goo, C. H. Kim, T. H. Kang, S. Y. Kim, S. J. Lee, S. H. Song, Y. M. Whang and Y. W. Choi (2019). "Intravesical delivery of rapamycin via folate-modified liposomes dispersed in thermo-reversible hydrogel." Int J Nanomedicine **14**: 6249-6268.
Zhan, Q., K. Yi, X. Li, X. Cui, E. Yang, N. Chen, X. Yuan, J. Zhao, X. Hou and C. Kang (2021). "Phosphatidylcholine-Engineered Exosomes for Enhanced Tumor Cell Uptake and Intracellular Antitumor Drug Delivery." Macromol Biosci **21**(8): e2100042.
Zoubari, G., S. Staufenbiel, P. Volz, U. Alexiev and R. Bodmeier (2017). "Effect of drug solubility and lipid carrier on drug release from lipid nanoparticles for dermal delivery." Eur J Pharm Biopharm **110**: 39-46.

FIGURE CAPTIONS AND TABLES

Figure 1. Influence of composition modification, sonication time and drug incorporation on the physicochemical characteristics of nanocarriers. (A) Influence of the type of liquid oil (tributyrin, TB, or tricaprylin, TC), oil phase surfactant type (span 80 or phosphatidylcholine, PC) and sonication time (10 or 20 min) on size, PDI and zeta potential of the NLC. (B) Influence of aqueous phase surfactant type (polysorbate 80 or decyl glucoside, DG) and concentration (1 or 3%, w/w) on size, PDI and zeta potential of the NLC. (C) Influence of the drug type (paclitaxel, P, or 5-fluorouracil, 5FU) and concentration (0.5 or 1%, w/w) on size, PDI and zeta potential of the NLC. * $p < 0.05$, ** $p < 0.01$, *** $p < 0.001$ and *** $p < 0.0001$.

Figure 2. Scanning Electron Microscopy images of (**A**) Unloaded nanocarriers, (**B**) Paclitaxel-loaded nanocarriers and (**C**) 5-Fluorouracil-loaded nanocarriers. The original scale bar is included in the images, but because of its reduced size, a white line with the same length as the original scale bar was included in all images to facilitate size estimation. Scale bar = 2 μm.

Figure 3. Thermogravimetric (TGA) and differential scanning calorimetry (DSC) curves of tributyrin, Compritol, paclitaxel, 5-fluorouracil, the physical mixtures of the different compounds and freeze-dried NLCs. NLC-TB: NLC containing tributyrin (TB) as liquid oil; NLC-TB-P: NLC containing tributyrin (TB) as liquid oil and paclitaxel; NLC-TB-5FU: NLC containing tributyrin (TB) as liquid oil and 5-FU.

Figure 4. Influence of nanocarrier composition and drug encapsulation on the cytotoxicity in (**A**) MCF-7, (**B**) T-47D, (**C**) MDA-MB-231 cells and (**D**) MCF-10A in 2D (monolayer) culture after 72 h of treatment. Data are represented as the mean ± SO, n = 8 – 12. The concentrations of the formulation and drugs, paclitaxel and 5-fluorouracil (5-FU), are represented in mg/mL and μM, respectively. NLC-TC: NLC containing tricaprylin (TC) as liquid oil; NLC-TC-P: NLC containing tricaprylin (TC) as liquid oil and paclitaxel; NLC-TC-5FU: NLC containing tricaprylin (TC) as liquid oil and 5-FU; NLC-TB: NLC containing tributyrin (TB) as liquid oil; NLC-TB-P: NLC containing tributyrin (TB) as liquid oil and paclitaxel; NLC-TB-5FU: NLC containing tributyrin (TB) as liquid oil and 5-FU; sol-P: solution of paclitaxel; sol-5FU: solution of 5-FU.

Figure 5. Influence of nanocarrier composition and drug encapsulation on cytotoxicity of (**A**) MCF-7 and (**B**) T-47D cells in 3D (spheroids) culture after 72 h of treatment. Data are

represented as the mean ± sd, n = 3 – 4. The concentrations of the formulation and drugs (paclitaxel and 5-FU) are represented in mg/mL and µM, respectively. NLC-TB: NLC containing tributyrin (TB) as liquid oil; NLC-TB-P: NLC containing tributyrin (TB) as liquid oil and paclitaxel; NLC-TB-5FU: NLC containing tributyrin (TB) as liquid oil and 5-FU; sol-P: solution of paclitaxel; sol-5FU: solution of 5-FU.

Figure 6. Morbidity (**A**) and survival (**B**) curves of *Galleria mellonella* larvae treated with nanostructured lipid carriers (NLC-TB) and PBS (negative control). ** $p < 0.01$ and *** $p < 0.001$ compared to negative control.

Figure 7. Characterization of the poloxamer dispersion containing NLC. Panels **A** and **B** depict the influence of NLC incorporation on the rheological behavior (**A**) and viscosity (**B**) of selected formulations at 25º (black circles) and 37 ºC (grey circles).

Figure 8. Drug release and stability upon short-term storage of selected formulations. Panel (**A**) shows the cumulative release of paclitaxel and 5-fluorouracil from nanocarriers and drug solutions as a function of time. Panel (**B**) represents the changes in size, polydispersity index and zeta potential of unloaded NLC (NLC-TB) and drug-loaded NLC (NLC-TB-P and NLC-TB-5FU for paclitaxel- and 5-Fluorouacil-loaded nanocarriers) over 60 days. Panel (**C**) represents changes on the encapsulation efficiency of paclitaxel and 5-fluorouracil for 60 days. Panel (D) represents the influence of NLC lyophilization and incorporation in poloxamer dispersion on size distribution, polydispersity index (PDI) and zeta potential for 60 days. ** $p < 0.01$, *** $p < 0.001$ and *** $p < 0.0001$ vs NLC-TB at day 0; ## $p < 0.01$ and ### $p < 0.001$ vs NLC-TB-P at day 0; and $$ $p < 0.01$ and $$$ $p < 0.001$ vs NLC-TB-5FU at day 0.

Figure 9. *In vivo* mammary retention of the fluorescent markers rhodamine ("R") and Alexa Fluor 647 ("A") over 120 h after intraductal (i.d.) or peritoneal (i.p) administration (**A**) Representative images of the fluorescence signal in Wistar female rats treated with solutions (Sol), nanostructured lipid carrier loaded with markers dispersed in water (NLC) or incorporated in poloxamer (named NLC Gel, considering the viscosity gain at physiological temperature); unloaded NLC was employed for autofluorescence assessment. (**B**) Decay of fluorescence intensity along 120 h after ID administration. **** $p < 0.0001$ compared to NLC Gel i.d.

Figure 10. Histological characteristics of breast tissue after treatment with experimental groups: (i) intraductal unloaded-NLC, (ii) intraductal Rhodamine-NLC (NLC-R), (iii) intraductal rhodamine-NLC incorporated in gel (NLC-R Gel), (iv) intraductal rhodamine solution (Sol-R) and (v) intraperitoneal NLC-R. HE stains and scale bar = 100 µm.

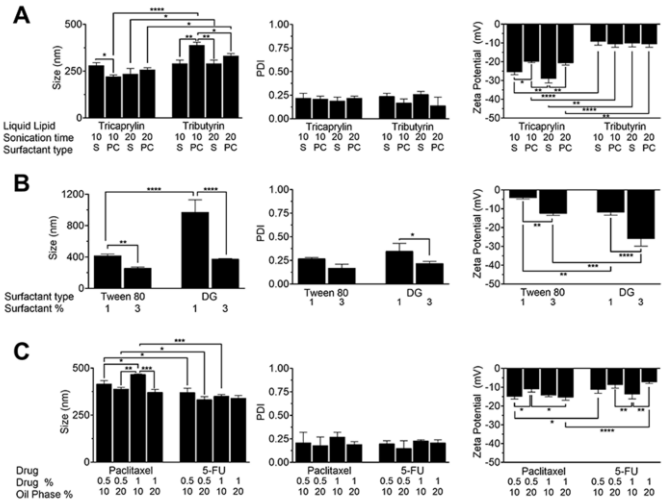

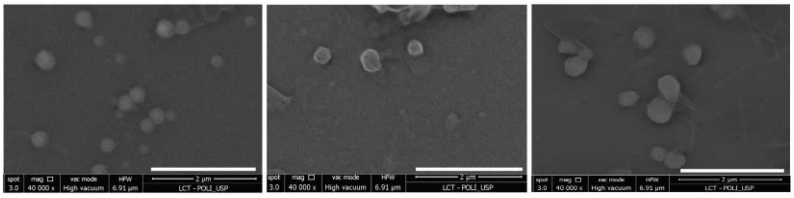

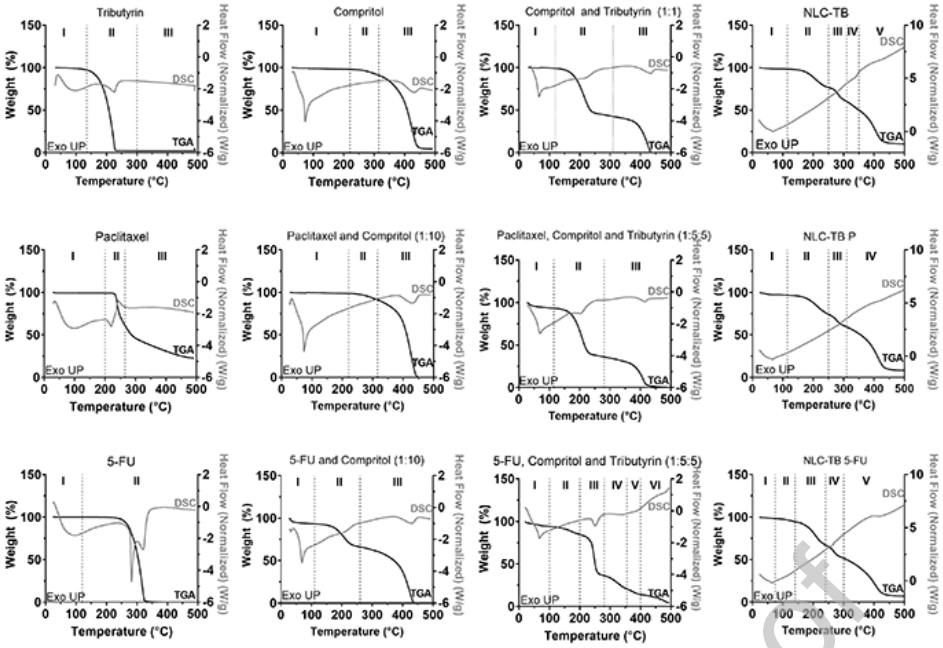

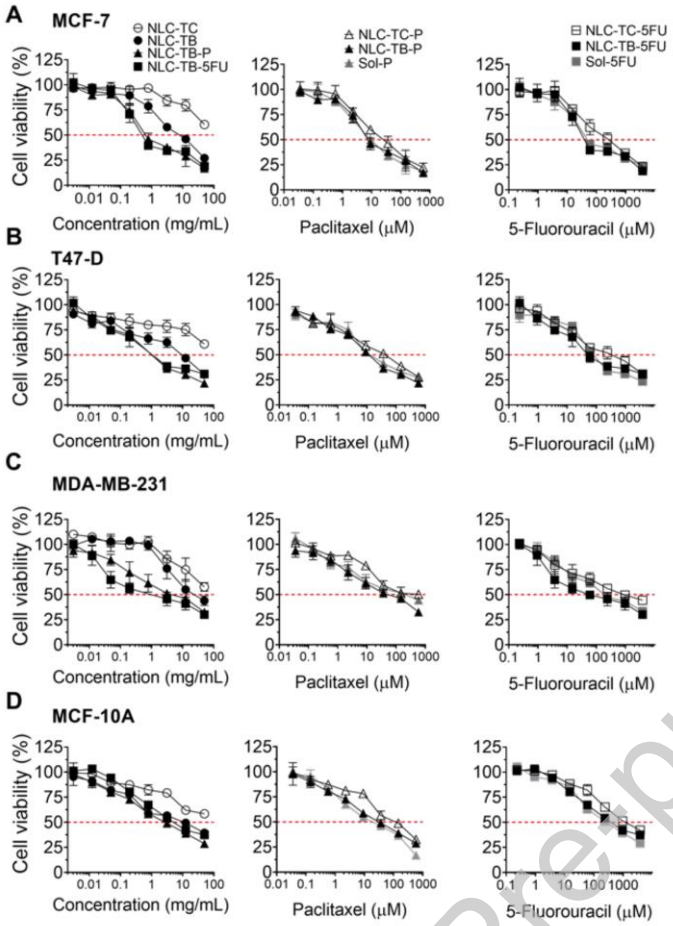

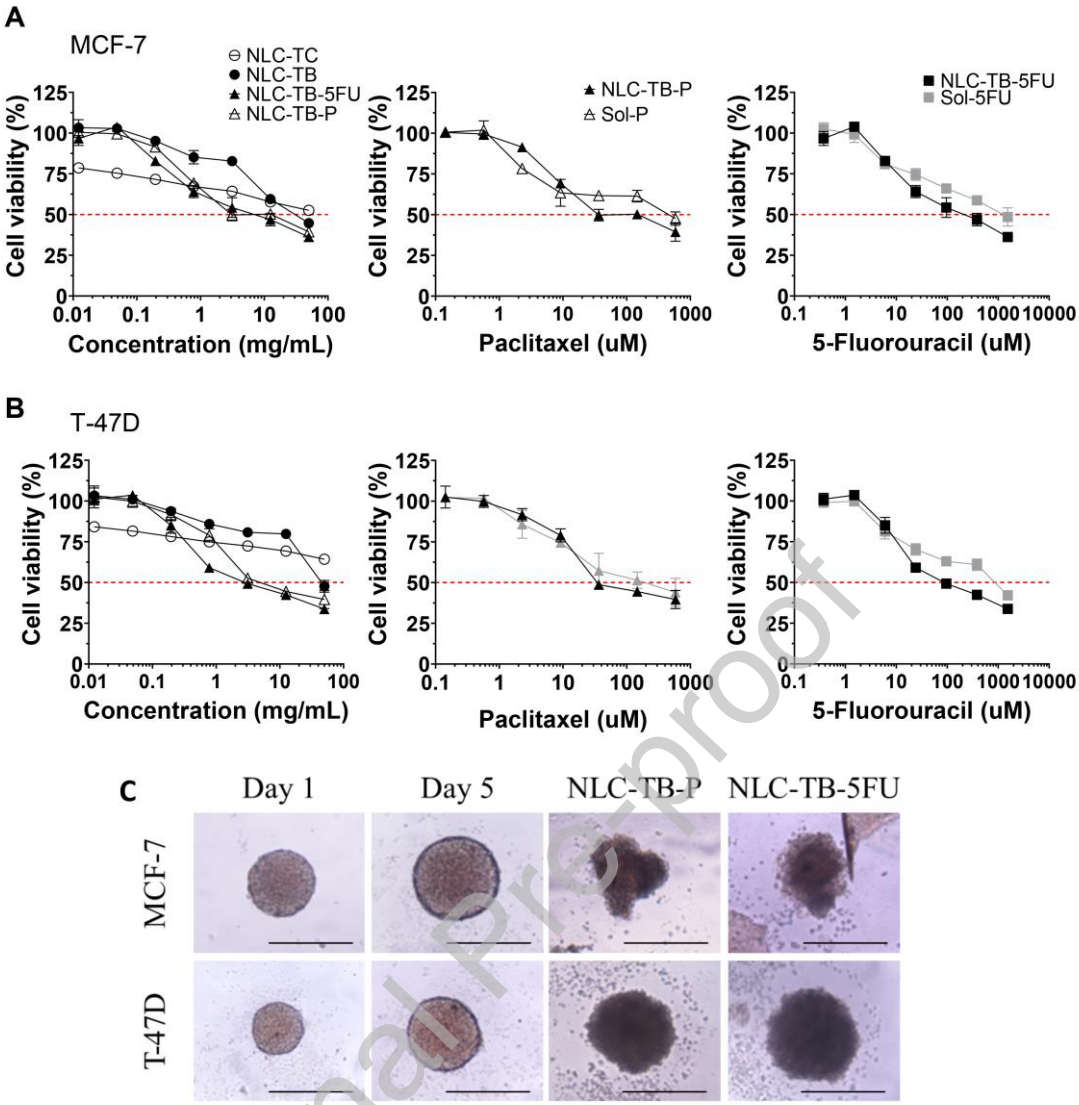

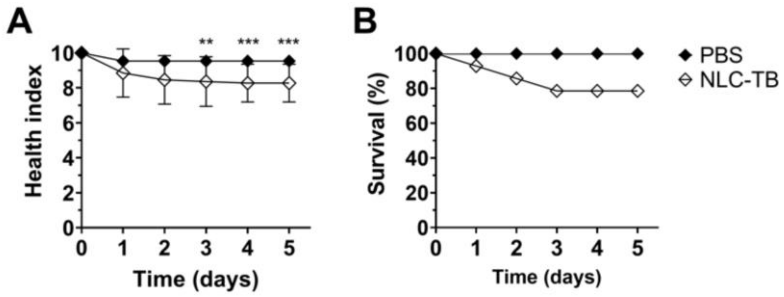

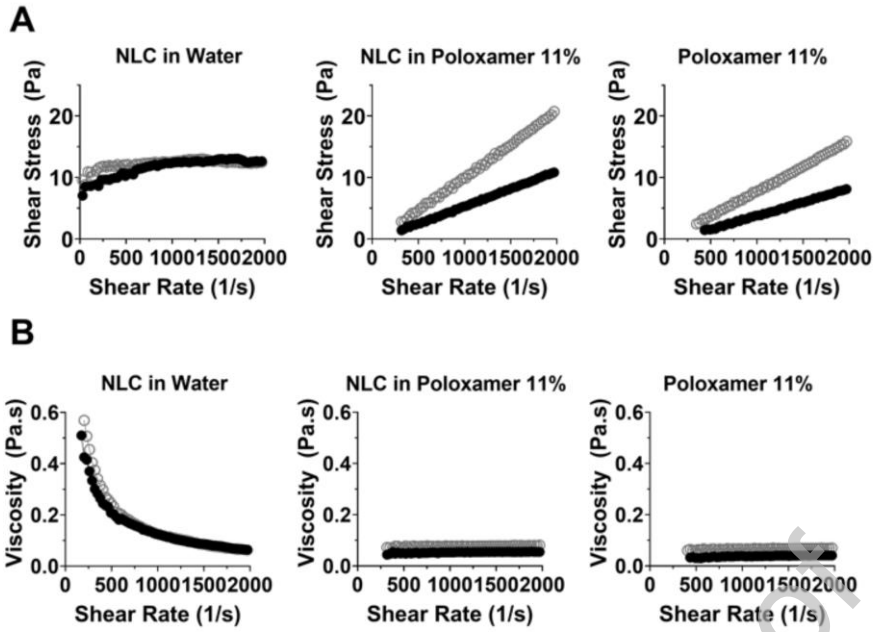

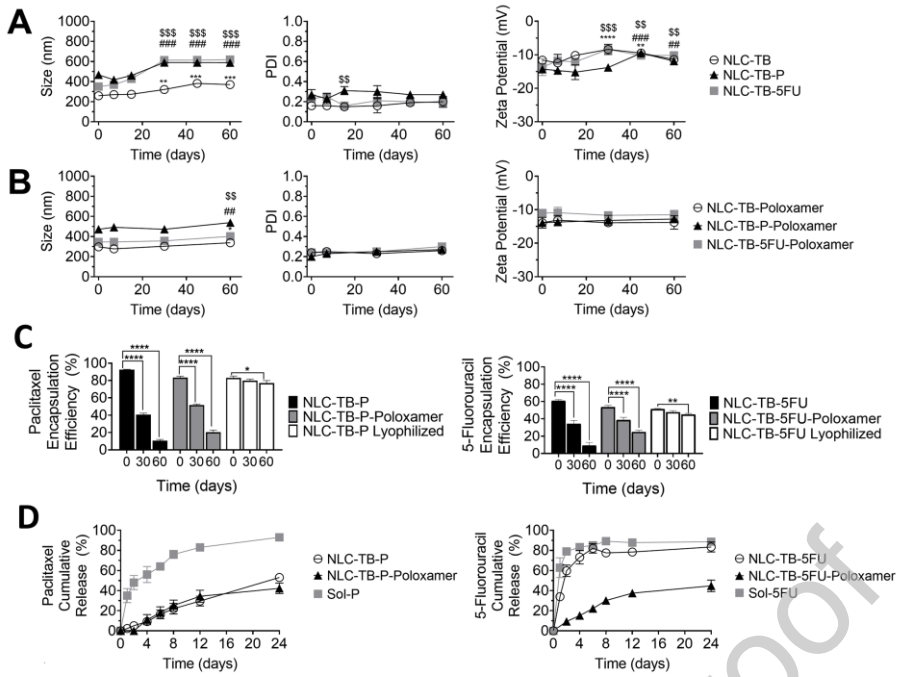

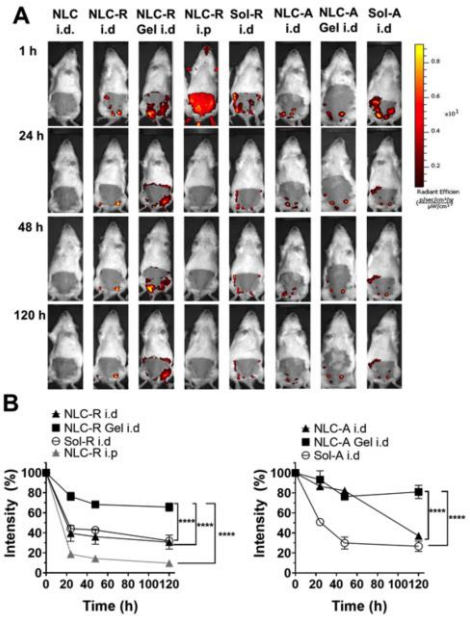

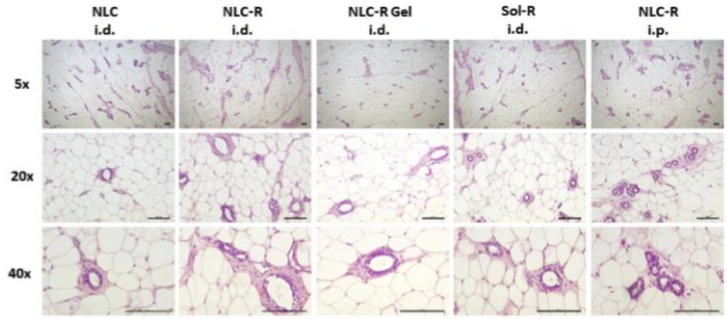

Table 1. Thermogravimetric analysis (TGA) and differential scanning calorimetry (DSC) data of the pure substances (tributyrin, compritol, paclitaxel and 5-fluorouracil), the physical mixtures of the different compounds and the selected nanostructured lipid carriers (drug-loaded and unloaded).

Sample	Step I					Step II					Step III, IV, V and VI					Residue (500 °C)
	ΔW (%) T Range (°C)	T_{onset} (°C)	T_{peak} DTG (°C)	T_{peak} DSC (°C)	ΔH (J/g)	ΔW (%) T Range (°C)	T_{onset} (°C)	T_{peak} DTG (°C)	T_{peak} DSC (°C)	ΔH (J/g)	ΔW (%) T Range (°C)	T_{onset} (°C)	T_{peak} DTG (°C)	T_{peak} DSC (°C)	ΔH (J/g)	ΔW (%)
TB	2.7 (25 - 135)	121.5		97.8	152.5	95.3 (135 - 300)	195.6	225.0	227.3	81.0	0.1 (300 - 500)	304.6				1.9
CP	1.9 (25 - 220)	95.0		73.5	80.0	7.0 (220 - 315)	266.9				86.7 (315 - 500)	390.7	423.0	430.9	59.8	4.4
CP + TB (1:1)	0.7 (25 - 120)	64.5		65.9	32.5	56.7 (120 - 310)	182.8	215.0			48.0 (310 - 500)	396.0	425.0	433.6	40.0	0
NLC-TB	1.4 (25 – 115)	25.3				21.8 (115 – 250)	173.1				III: 16.7 (250 – 310) IV: 10.7 (310 – 350) V: 39.3 (350 – 500)	III: 269.3 IV: 323.0				10.1
Paclitaxel	0.6 (25 - 200)	30.7		94.6	176.3	38.2 (200 - 265)	234.3		(I) 220.5 (II) 243.6	(I) 29.0 (II) 47.6	37.4 (265 - 500)	272.8				23.8
5-FU	0.5 (25 - 120	24.4		86.1	271.6	101.6 (120 -	290.5		(I) 282.2 (II)	(I) 113.3 (II)						0

	)					500)			32 0.9	48. 6						
Paclitaxel + CP (1:10)	1.2 (25 - 220)	78. 1		73. 7	10 2.1	7.4 (22 0 - 315)	26 6.9				92.7 (31 5 - 500)	39 7.2	42 5.0	43 0.6	10 4.5	0
Paclitaxel + CP + TB (1:5:5)	6.8 (25 - 115)	30. 5		70. 6	90. 5	57.2 (11 5 - 280)	17 8.4	20 7.0			35.8 (28 0 - 500)	38 3.9	41 0.0	41 4.7	27. 0	0.2
NLC-TB P	3.2 (25 – 115)	24. 7				22.6 (11 5 – 250)	17 6.4				III: 14.9 (25 0 – 310) IV: 51.1 (31 0 – 500)	III: 26 6.2 IV: 38 3.4				8.2
5-FU + CP (1:10)	6.3 (25 - 110)	30. 8	31. 0	I: 32. 7 II: 68. 8	I: 6.6 II: 61. 8	27.2 (11 0 - 260)	17 4.9	20 7.0			70.9 (26 0 - 500)	38 8.0	42 1.0	43 1.2	65. 4	0
5-FU + CP + TB (1:5:5)	5.2 (25 - 100)	21. 1		67. 1	31. 3	9.4 (10 0 - 200)	14 5.1				III: 48.4 (20 0 - 280) IV: 15.6 (28 0 - 355) V: 6.5 (35 5 - 400) VI: 10.0 (40 0 - 500)	III: 23 7.9 IV: 30 2.2 V: 26 8.5 VI: 45 2.3	III: 24 6.0 IV: 32 6.0 V: 37 8,0 VI: 47 8,0	III: 25 1.1	III: 36. 5	4.9
NLC-TB 5-FU	1.7 (25 – 75)	23. 3				3.6 (75 – 140)	10 2.4				III: 27.5 (15 0 – 240	III: 18 0.1 IV: 26				7.0

											) IV: 16.0 (240 – 300) V: 44.0 (300 – 500)	0.6 V: 373.4				

T range = Temperature range, DTG = derivative thermogravimetry, ΔH = enthalpy (normalized), Tonset = onset temperature, T_{peak} = peak temperatute, TB = Tributyrin, CP = Compritol, P = Paclitaxel, 5-FU = 5-Fluorouracil, NLC-TB: NLC containing tributyrin as liquid lipid, NLC-TB-P: NLC containing tributyrin as liquid lipid and paclitaxel, NLC-TB-5FU: NLC containing tributyrin as liquid lipid and 5-FU.

Table 2. Values of IC50 related to MCF-7, T-47D, MDA-MB-231 and MCF-10A cell lines cultured in monolayer (2D model) or spheroids (3D model).

Treatment	**Drug**	**MCF-7**				**T-47D**				**MDA-MB-231**		**MCF-10A**	
		IC50 (mg/mL, (formulation)		**IC50 (µM, drug)**		**IC50 (mg/mL, formulation)**		**IC50 (µM, drug)**		**IC50 (mg/mL, formulation)**	**IC50 (µM, drug)**	**IC50 (mg/mL, Formulation)**	**IC50 (µM, drug)**
		Monolayer	**Spheroid**	**Monolayer**	**Spheroid**	**Monolayer**	**Spheroid**	**Monolayer**	**Spheroid**	**Monolayer**		**Monolayer**	
NLC TB	-	7.8	30.7	-	-	7.1	58.9	-	-	24.6	-	8.6	-
NLC TC		-	-	-	-	-	-	-	-	-	-	-	-
NLC TB	**Paclitaxel**	1.3	9.7	14.9	49.37	1.1	9.7	15.1	54.57	5.0	58.4	3.1	36.2
NLC TC		2.6	-	30.6	NE	3.3	-	40.0	NE	23.2	353.5	9.0	106.1
Solution		1.3	25.9	15.4	303.5	1.7	19.4	17.9	174.7	11.8	120.1	2.0	22.0
NLC TB	**5-FU**	1.3	7.8	83.2	239.2	1.4	5.2	107.7	161.9	1.6	80.3	6.9	507.3
NLC TC		3.6	-	274.9	NE	3.7	-	284.0	NE	11.3	867.2	17.4	1042.0
Solution		1.6	30.0	100.8	932.2	1.5	21.3	118.9	655.2	3.5	128.0	4.8	356.0

NE = not evaluated

Graphical abstract